PETROGRAPHY AND CHEMICAL COMPOSITION OF THE TRACE FOSSIL *OPHIOMORPHA NODOSA* IN NANGANG FORMATION, NORTHEAST COAST OF TAIWAN

Mr. Patthapong Chaiseanwang

A Report Submitted in Partial Fulfillment of the Requirements for the Degree of

Bachelor of Science

Department of Geology

Faculty of Science

Chulalongkorn University

Academic Year 2017

ศิลาวรรณนาและองค์ประกอบทางเคมีของซากดึกดำบรรพ์ร่องรอย *Ophiomorpha nodosa* ในหมวดหินนันกัง บริเวณชายฝั่งตะวันออกเฉียงเหนือของประเทศไต้หวัน

นายปัฐพงศ์ ไชยแสนวัง

รายงานฉบับนี้เป็นส่วนหนึ่งของการศึกษาตามหลักสูตรปริญญาวิทยาศาสตร์บัณฑิต
ภาควิชาธรณีวิทยา คณะวิทยาศาสตร์ จุฬาลงกรณ์มหาวิทยาลัย
ปีการศึกษา 2560

Title: PETROGRAPHY AND CHEMICAL COMPOSITION OF THE TRACE FOSSIL *OPHIOMORPHA NODOSA* IN NANGANG FORMATION, NORTHEAST COAST OF TAIWAN

Researcher: Patthapong Chaiseanwang **Student ID:** 5732734323

Advisor: Dr. Sakonvan Chawchai **Co-advisor:** Assoc. Dr. Ludvig Löwemark

Department: Geology **Academic year:** 2017

Trace fossils provide a geological record of biological activity and are able to indicate changes in the depositional environment. Trace fossils including a burrow system of *Ophiomorpha* generated by crustaceans are common in outcrops along the northeast coast of Taiwan. These trace fossils are often preferentially preserved in the outcrops, indicating a different mineral composition in comparison to host sediments. Therefore, this study investigated geochemical aspects of the differential diagenesis of trace fossils and surrounding host sediment. Several sandstone samples were collected showing preservation of the trace fossil in epirelief (i.e., more resistant than surrounding rock) and hyporelief (i.e., less resistant than surrounding rock), in the same sedimentary succession. Geochemical investigation was performed using petrographical thin-sections, Itrax XRF core scanning of rock slab samples that were cut perpendicular through *Ophiomorpha nodosa* burrows. Also, XRF and XRD are conventionally used for spot analysis of powdered-samples in order to observe chemical and mineralogical compositions respectively. Based on observations made in this study, samples of trace fossil preserved both in epirelief and hyporelief are mainly composed Iron (Fe) that found Goethite (FeO(OH)). Similarly, they have low contents of Silicon (Si), Aluminum (Al), and Potassium (K) that found Quartz (SiO_2), Feldspar ($KAlSiO_2$) and Illite-mica ($(Al,Mg,Fe)_2(Si,Al)_4O_{10}[(OH)_2,(H_2O)]$). The main difference between two types is petrography that the trace fossil in hyporelief were finer-grained and more matrix-supported compared to the trace fossil in epirelief under microscope. These observations lead to a preliminary interpretation for this study area that the preservation of *Ophiomorpha nodosa* is related to diagenetic mineralization of the burrow walls, causing differential erosion and weathering. Trace fossils that is grain-support and less matrix are often preferentially preserved, while trace fossils with more matrix-support are preferentially eroded.

Keywords: *Ophiomorpha nodosa*, Diagenesis, Burrow walls

หัวข้องานวิจัย: ศิลาวรรณนาและองค์ประกอบทางเคมีของซากดึกดำบรรพ์ร่องรอย *Ophiomorpha nodosa* ในหมวดหินนันกัง บริเวณชายฝั่งตะวันออกเฉียงเหนือของประเทศไต้หวัน

ผู้ทำการวิจัย: นายปัฐพงศ์ ไชยแสนวัง **รหัสประจำตัวนิสิต:** 5732734323

อาจารย์ที่ปรึกษา: ดร. สกลวรรณ ชาวไชย

อาจารย์ที่ปรึกษาร่วม: Assoc. Dr. Ludvig Löwemark

ภาควิชา: ธรณีวิทยา **ปีการศึกษา:** 2560

ซากดึกดำบรรพ์ร่องรอยจัดเป็นหลักฐานทางธรณีวิทยาที่เกิดจากการกระทำของสิ่งมีชีวิตและบ่งบอกสภาพการสะสมตัวของสิ่งแวดล้อมในอดีตโดย *Ophiomorpha nodosa* เป็นซากดึกดำบรรพ์ร่องรอยประเภทรูชอนไชที่เกิดจากสัตว์จำพวกครัสเตเชียน (Crustacean) ซึ่งจะพบมากบริเวณชายฝั่งตะวันออกเฉียงเหนือของประเทศไต้หวัน โดย *Ophiomorpha nodosa* ที่พบในบริเวณนี้ถูกเก็บรักษาอยู่ในชั้นหินทรายที่มีองค์ประกอบของแร่ที่แตกต่างจากหินทรายโดยรอบ จึงทำให้เกิดการศึกษาธรณีเคมีเพื่อดูความแตกต่างของกระบวนการก่อตัวใหม่ระหว่างซากดึกดำบรรพ์ร่องรอยกับหินทรายโดยรอบ ซึ่งตัวอย่างหินที่พบ *Ophiomorpha nodosa* ถูกนำมาเป็นตัวอย่างในงานวิจัยโดยลักษณะปรากฏของตัวอย่างแรกพบ *Ophiomorpha nodosa* ที่แข็งแรงกว่าหินทรายโดยรอบ (Epirelief) แตกต่างกับอีกตัวอย่างที่หินทรายโดยรอบแข็งแรงกว่า (Hyporelief) ซึ่งตัวอย่างทั้งสองอยู่ในชั้นหินทรายเดียวกัน เทคนิคการทำแผ่นหินบางถูกนำมาใช้ศึกษาลักษณะทางศิลาวรรณนาและ Itrax XRF core scanning นำมาประยุกต์ใช้ในการศึกษาธรณีเคมีโดยการวิเคราะห์จากตัวอย่างที่เป็นแผ่นหินที่ตัดผ่าน *Ophiomorpha nodosa* อีกทั้งใช้หลักการวิเคราะห์ธาตุองค์ประกอบและแร่องค์ประกอบเฉพาะจุดโดยใช้ XRF และ XRD จากการศึกษาพบว่า *Ophiomorpha nodosa* ของตัวอย่างทั้งสองส่วนใหญ่ประกอบด้วยธาตุเหล็กปริมาณมากนั่นคือการพบแร่เกอไทต์ (FeO(OH)) แต่ธาตุซิลิกอน อลูมิเนียม และโพแทสเซียมพบในปริมาณน้อยจากการพบแร่ควอตซ์ (SiO_2) แร่เฟลสปาร์ ($KAlSiO_2$) แร่อิลไลต์-ไมก้า ($(Al,Mg,Fe)_2(Si,Al)_4O_{10}[(OH)_2,(H_2O)]$) ซึ่งความแตกต่างของสองตัวอย่างอยู่ที่ลักษณะทางศิลาวรรณนาภายใต้กล้องจุลทรรศน์พบว่าตัวอย่าง Hyporelief มีเม็ดละเอียดมากกว่าและมีเนื้อพื้นสูงกว่าเมื่อเทียบกับลักษณะศิลาวรรณนาของตัวอย่าง Epirelief ทำให้สามารถแปลความหมายได้ว่า *Ophiomorpha nodosa* ที่ถูกเก็บรักษาไว้ในชั้นหินทรายนี้สัมพันธ์กับกระบวนการก่อตัวใหม่ของแร่ที่ทำให้เกิดความแตกต่างในการกัดกร่อนและการผุพัง โดยซากดึกดำบรรพ์ร่องรอยที่มี grain-support ที่มากกว่าจะปรากฏลักษณะร่องรอยที่เด่นชัด ในขณะที่ซากดึกดำบรรพ์ร่องรอยที่มี matrix-support จะถูกกัดกร่อนหายไป

คำสำคัญ: *Ophiomorpha nodosa*, กระบวนการก่อตัวใหม่, ซากดึกดำบรรพ์ร่องรอย

ACKNOWLEDGEMENTS

First, I would like to thank DPST for giving me a chance to go to exchange new experience in Taiwan. I also thank for both my advisor and my co-advisor who guide my field observation, my senior project and always take care me during the whole time in Taiwan. Furthermore, my new Taiwanese friends always help my work, enjoy life together.

I am really thankful to Department of Geosciences, National Taiwan University. I am supported by Ludvig Lowemark's team (my co-advisor) including of Chung-Ping, Tsai-wen, Boris, and many more. Giving me new experience, supporting of analysis that help my project.

I appreciate to have Dr. Sakonvan Chawchai as my advisor. She always guides my work, be like a sister who take care and treat me very well. She also dedicates her time to be the best advisor.

Finally, my supports come from my family and my friends (Geo'58). Especially, my advisor's team including of Poom, White, Gift, and Nard who have passed through and enjoyed working together along this journey.

TABLE OF CONTENTS

LIST OF TABLES

LIST OF FIGURES

FIGURE **Page**

Chapter 1

Introduction

1.1 Rationale

Trace fossil is a geological indicator for biological activities formed by animals, for example; borings, burrows, footprints, including organic matter (i.e., coprolite). Trace fossil shows not only morphological evidence but also activities of animals in the past (Tonsatian, 2006). A study of trace fossil is called Ichnology, which relates to animals' behavior in certain environment. Moreover, the study of trace fossil is an interaction of organism with environment and ecology of each organism which is important to apply for sedimentology and stratigraphy. Since the response of trace fossil for each environments or events happened in the past can be disclosed the environmental factors control behavior such as velocity of stream or tide, water depth, fluid flow, nutrient content (Ekdale and Mason, 1988) . Therefore, trace fossil is one of paleoenvironmental indicator and can be used for studying of paleoecology (Tonsatian, 2006).

The trace fossil *Ophiomorpha* is one of burrows which is generally formed by crustaceans group. These species are diverse in taxonomy, some have pellet outside but some have not. Some species of *Ophiomorpha* was formed in certain place in the past. Thus, paleoenvironment and depositional environment can be indicated where *Ophiomorpha* is found, for example; one of the deepest burrows in deep-sea sandy sediments is characterized by *Ophiomorpha rudis*. (Uchman, 2009). Alternatively, trace fossils are helpful for indicating sedimentary facies instead of the study of body fossils. Seilacher (1964) used trace fossil associations (ichnofacies) to determine sedimentary facies. After that Frey et al. (1990), Bromley and Asgaard (1991) created primarily model of relation of energy changes in marine environment and ichnofacies (i.e. deep marine environment is characterized by *Nereites* ichnofacies). Similarly, *Ophiomorpha nodosa*

that appears on sedimentary succession can indicate nearshore environment (Frey et al., 1978).

Nangang Formation in Miocene epoch on Yehliu Group is commonly found in the northern part of Taiwan. The Nangang Formation is characterized by shallow marine environment, mostly sandstone succession, sandstone interbedded shale, which deposited during transgressive period (Chou, 1970; Hong and Wang, 1988; Huang, 1990). The thickness of the Formation is about 500 m.

In Miocene sandstone, Nangang Formation on the northeast coast of Taiwan, burrows and crustacean subphylum can be commonly found. The study of Löwemark et al. (2016) discovered that *Ophiomorpha* in sedimentary succession has a feature of Inner tube inside them. Accordingly, physical feature, size, thickness of both tubes of *Ophiomorpha* and stratigraphic column, bedding and cross-section are reported. Over hundred specimens were investigated for creating 3D of *Ophiomorpha* model.

From the field survey, Riubin's gulf on the northeast coast of Taiwan (Fig. 1.1 and Fig 1.2), there are *Ophiomorpha nodosa* preserved in epirelief (i.e. more resistant than surrounding rock) and hyporelief (i.e. less resistant than surrounding rock), in the same sedimentary succession. This infer to differential preservation which may relate to the different in weathering process and/or diagenesis. To better understand how *Ophiomorpha nodosa* preservation can be related to this process, the aim of this study is to study chemical and minerals compositions of *Ophiomorpha nodosa* by applying non-destructive ITRAX XRF core scanning method (Croudace and Rothwell, 2010), petrography and XRD analysis, respectively.

1.2 Objective

To compare petrography and chemical composition of the different preservation of *Ophiomorpha nodosa* in Nangang Formation, Northeast coast of Taiwan.

1.3 Study area

The study area is a small islet around Riubin's gulf located on northeast coast of Taiwan (25.125560°N and 121.819113°E). It is about 20 km. southeast from well-known Yehliu Geopark.

Figure 1.1 (A) Study area locates on Riubin's gulf, northeast coast of Taiwan. The red star locates the study area. Overlap with geological map that Nangang Formation displays on blue area. Faults and minor faults show on the black line. (B) Map of Taiwan where the red square locates study area (Modified from http://gis.moeacgs.gov.tw and google earth).

1.4 General geology (Data from the central geological survey (CGS))

Taiwan is located between collision of the Eurasian plate and the Philippine Sea plate. There is an oblique collision that begins on north toward south. The result of collision is north-south arc and northeast-southwest continental margin.

Geological provinces of Taiwan comprise of 3 zones eastern range, central range, and western foothills. Western foothills (Fig. 1.2) where is provided on late Cenozoic sedimentary basin west of Central range with including Penghu Islands and Hengchun Peninsula. Littoral to shallow marine depositional environment is defined for this geological province that form Oligocene to Neogene rocks based on the study of planktonic foraminifers and calcareous nannofossils.

General stratigraphy of the western foothills consists of Oligocene rocks, Miocene rocks, Pliocene rocks and Quaternary rocks. In this study, we focused on Miocene rocks that are mainly composed of shallow to nearshore sedimentary deposits, mostly sandstone, siltstone, shale and some distribution of carbonate reefs and lenticular tuff. These strata are variable in thickness by increasing eastward cause of asymmetrical sedimentary basin. On the northern part of Taiwan, the Miocene rocks are comprised of three sedimentary cycles that can be divided into early, middle, and late by chronology. Each cycle has one coal-bearing formation and one marine unit. The lower part is Yehliu Group, that is absent in the southern Taiwan but thicker and more finer compare to the north, underlying on the middle Jiufang Group and upper Sanhsia Group, respectively. Lateral facies changes are common in these strata that gradually change in both lithological character and stratigraphic thickness from north toward south thus making more complex to defined sedimentary successions.

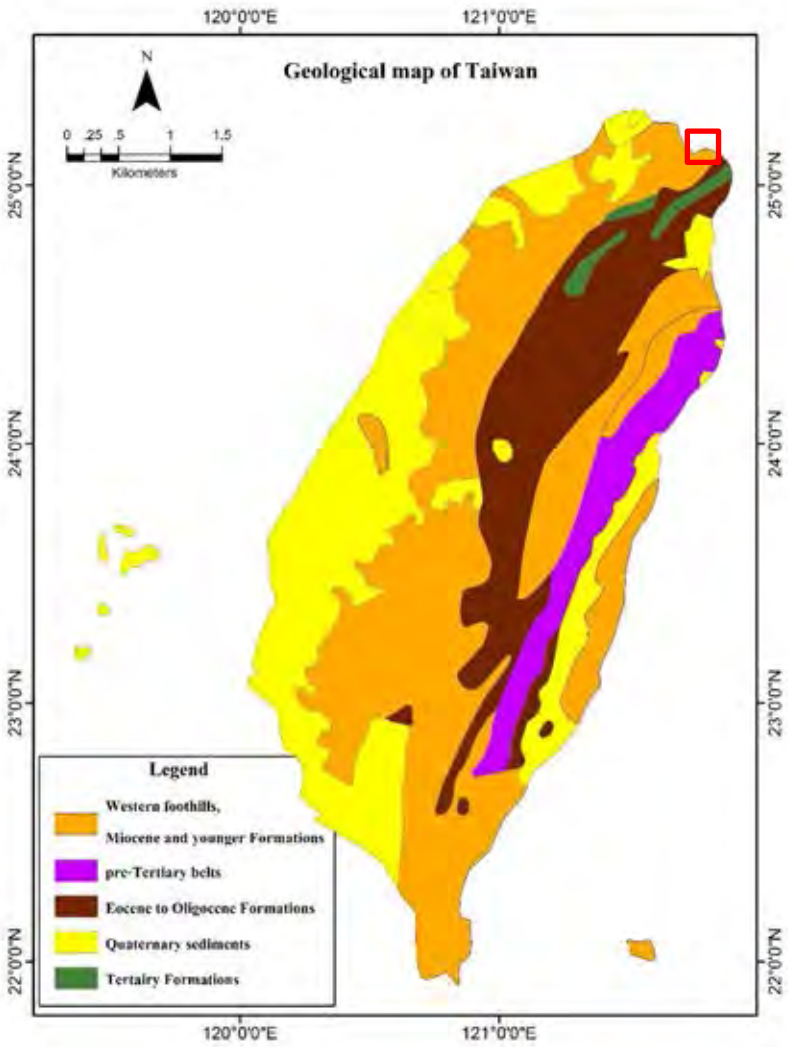

Figure 1.2 Geological map of Taiwan. The red square locates study where is on Western foothills, Miocene and younger Formations (Orange color)

Nangang Formation

The study area is located on the northeastern coast in strata of the Nangang Formation which overlying the Shihti Formation and underlying the Nanchuang Formation in Miocene rocks (Fig. 1.3). Type locality of this formation is located on eastern side of Nangang city, a large town between Taipei and Chilung. Shallow neritic depositional environments can be characterized on thick- to thin-bedded, light bluish gray, fined-grained calcareous sandstone and dark gray shale or siltstone with fossils of foraminifers and mollusks. This formation consists of two massive sandstone members

and three sandstone-shale members, mainly is lithic greywacke or sub-greywacke. In the northern Taiwan, Nangang Formation is distinctive cliff-forming sandstone due to lateral facies change and variation of sandstone-shale ratio. Five members in northern part can be changed into three members in central part and absence of members somewhere in southern part (Central geological survey).

The Nangang Formation is deposited during the transgressive period (Löwemark et al., 2016). On the northeast coast, there are seven small periods of transgressive-regressive cycles (Yu and Teng, 1996). This locality is also well exposed which make it easy to study.

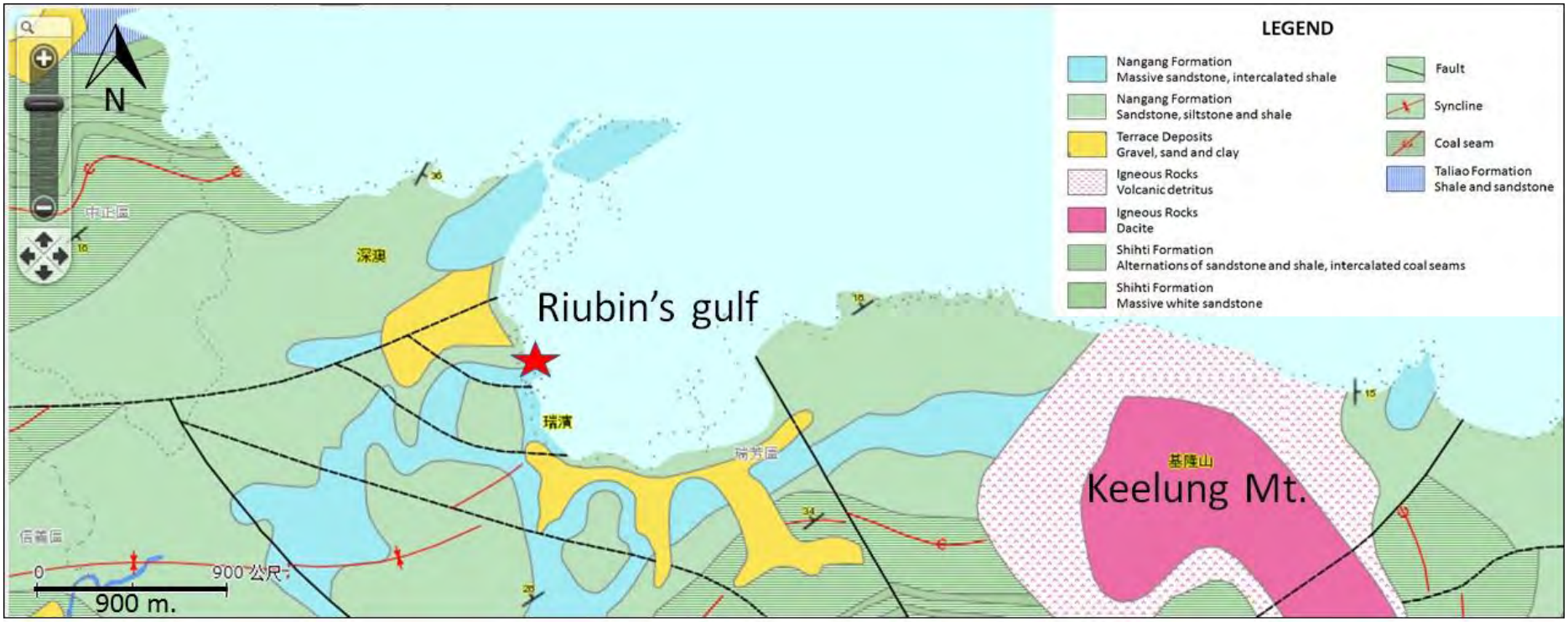

Figure 1.3 Geological map on northeast coast of Taiwan and Nangang Formation's distribution is showed on sky-blue and greenish-blue colors. The red star displays the study area. (Modified from http://gis.moeacgs.gov.tw).

1.5 Literature reviews

1.5.1 Taxonomy

Ophiomorpha is defined as trace fossils in the past, whereas burrows of *Callianassa* major are recent burrows. Many studies on taxonomy of trace fossils provide the basic for diagnosing ichnogenus of *Ophiomorpha*. Some studies discussed that the first prior consideration for taxonomic ichnogenus is pellets arrangement of burrow lining (Bromley and Frey, 1974). However, for individual specimens and environmental interpretation, more studies focus on geometric configuration of burrows system instead (Herreid and Gifford, 1963).

Examples of taxonomic ichnogenus definition, *Ophiomorpha*, Permian to Holocene (Lundgren 1891, Chamberlain and Bear, 1973), is diagnosed as simple to complex burrows system, having pellets and smooth inside wall. These trace fossils commonly occur in siliceous and calcareous sedimentary rocks, including chalk (Bromley and Frey, 1974; Kennedy, 1975).

Ophiomorpha nodosa consist of dense, discoid, ovoid, or irregular polygonal pellets on burrow walls (Lundgren 1891). These trace fossils widely occur with *Ophiomorpha irregulaire* and *Ophiomorpha borneesis* (Cheng, 1972).

1.5.2 Morphology of *Ophiomorpha*

The study of taxonomic concept of *Ophiomorpha* by Frey et al. (1978) defined that *Ophiomorpha* is clear burrows lining which has smooth interior wall but knobby wall on outside and knobs can be single, double, or irregularly formed pellets. The thickness of burrow lining is variable. These pellets are formed by animals, in order to support burrows wall and easier to remove sediments during burrows penetration (or feeding activity). However, pellet forms, are responded by behavioral patterns, still have less information.

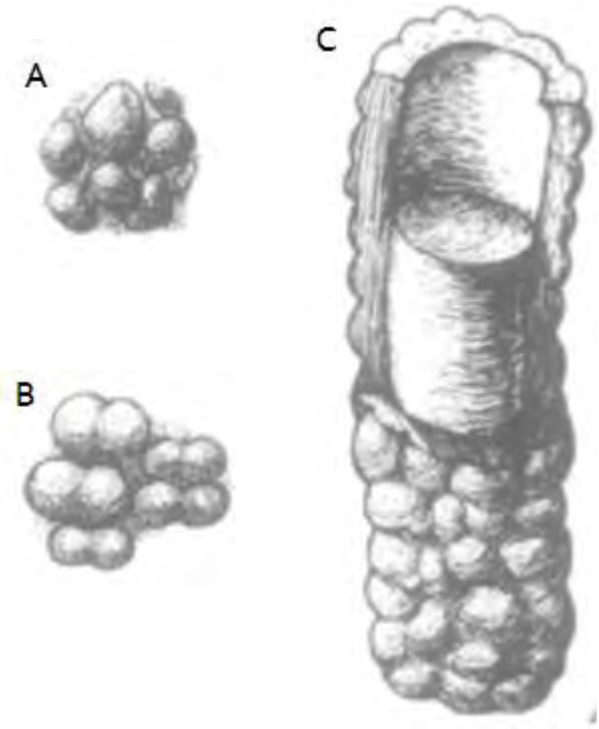

Figure 1.4 (A) Single formed pellets (B) Double formed pellets (C) *Ophiomorpha*'s burrows lining shows smooth interior wall and knobby exterior wall. Sediment is filled inside (Modified from Frey et al., 1978).

The burrows system of *Ophiomorpha* is variable. There are many burrows constructed names. For instance, component of shafts, tunnels or complex of these can be classified as shafts, mazes, and boxworks, respectively (Frey et al., 1978). They also have branches within system which typically have acute angle. On the variations in burrows morphology, the recent study found that the horizontal burrows have well knobby walls on the top but flat walls on the ground. Similarly, vertical and/or inclined burrows have thicker and more knobby walls in the upper part compare to the lower one. Therefore, they have high resistance for keeping wall above or next to the penetration.

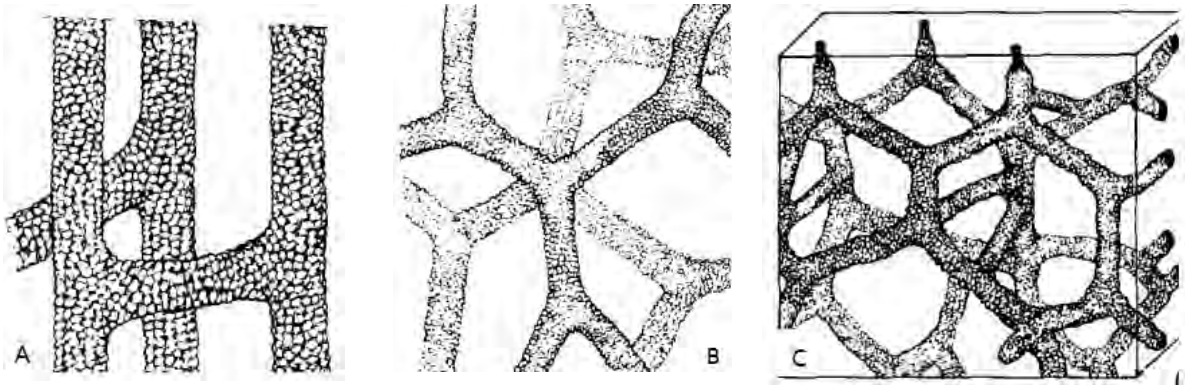

Figure 1.5 Burrows systems of *Ophiomorpha*. (A) Shafts (B) Mazes (C) Boxworks. (Modified from Frey et al., 1978).

1.5.3 Structure and composition of the burrows lining

The knobby walls of *Ophiomorpha* are composed of pellets which are typically sandy sediment and have c. 2-4 mm. in average diameter (Up to 1 cm.). Most walls are one-pellet-thick that means single-pellet wall construction. The interior of burrow has flat pellets and clayey sediment coated on them. There is a fine, circular or oval shape on cross-sections of burrows. Compaction of sediment is forced and formed by animals.

In thin-section, *Ophiomorpha* is easily recognized. Pellets are composed of large number of smaller pellets. These smaller pellets consist of fine matrix and sand-size grains set with 0.25-0.5 mm. in diameter. The grains are radial or concentric arrangement, mostly quartz, but individual pellets may consist of heavy mineral. Similarly, 60-75% is a fine matrix and sand-size grain float in matrix. Composition of the matrix, or cement vary with clay minerals, iron oxides and sulfides. The diagenetic effects are important in preservation of them. For instance, many specimens the presenting cement is not differ from siliceous or calcareous cemented host sediment cause of diagenetic diffusion the outside particles can join in burrow wall's component (Frey et al., 1978).

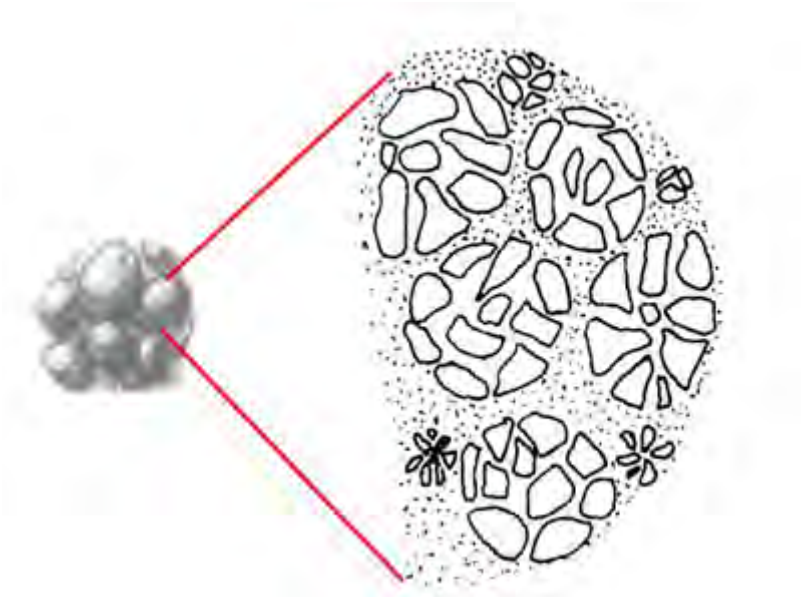

Figure 1.6 Pellets of *Ophiomorpha* are zoomed in under microscope. There are composed of many small pellets and contactless grains. (Modified from Frey et al., 1978)

1.5.4 The use of Ophiomorpha (Frey et al., 1978)

The study of *Ophiomorpha* is a key to indicate sediment reworking, substrate coherence, erosion, deposition, and geochemistry of sediments. Besides the physical study, *Ophiomorpha* is used to help improving sedimentary structures where are lack of them by observing on its morphology. This study can be inferred that burrows can be used for dividing boundaries of each sedimentary succession which is very similar and giving detailed stratigraphic columns. For paleoenvironment, *Ophiomorpha* is an implication for beaches, beach-like, shallow deposits indication high energy.

1.5.5 Itrax XRF core scanner and wavelength-dispersive X-ray fluorescence spectrometry (WD-XRF) (Croudace and Rothwell, 2010)

Itrax XRF core scanner, which was used for sediment core for the first time in paleoclimate research. In this study, we apply XRF core scanner for using in thin-slabbed sedimentary rock (i. e. sandstone) to observe continuously elemental compositions. This tool can rapidly analyze sample in high resolution with no destruction. Itrax XRF core scanner consists of X-ray fluorescence spectrometry (XRF)

which can detect many elements (Al to U) with part per million unit (ppm) on detection limit, a moveable detector, X-ray capillary waveguide, and cameras of optic and radiography which provide image for easily interpreting layers and grains of sedimentary rocks. Moreover, we also use conventional tools, wavelength-dispersive X-ray fluorescence spectrometry (WD-XRF) to compare chemical composition with the Itrax and also spot analysis which can pick interested spots for more precise analysis. Similarly, mineralogical study is observed by XRD and petrography. In this study, *Ophiomorpha*-dominated sandstone is analyzed for studying geochemistry (elemental composition and mineralogy).

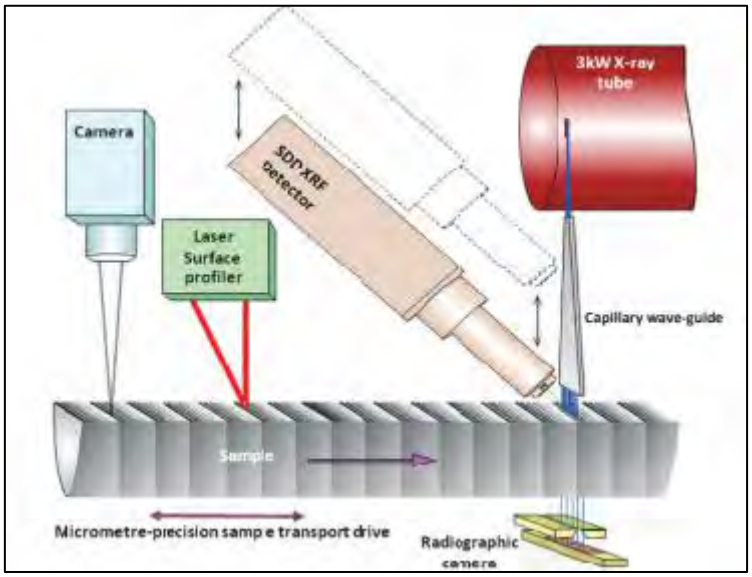

Figure 1.7 Schematic of Itrax XRF core scanner shows main components. (Modified from Croudace and Rothwell, 2010)

Chapter 2

Methodology

2.1 Geologic survey and collecting sample

The study area is in Ruifang district, Taipei city, Taiwan (Fig.2.1). It is a small islet in Riubin's gulf along the northeastern coast. Mostly, sandstone lies on subhorizontal dipping, intercalated with shale. The succession of study area is syncline and has minor faults nearby (Fig. 1.3) but no river dominates on the area.

In this study, we investigate outcrops of *Ophiomorpha*-dominated sandstone and collect samples by using automatic chainsaw, chisel and hammer. Samples selection are based on positioning in horizon, species of *Ophiomorpha nodosa* and appearance of *Ophiomorpha nodosa* preservation (Fig. 2.3).

Figure 2.1 Outcrop of sandstone in the study area.

Figure 2.2 Equipment consists of automatic chainsaw (lubricated by water), chisel and hammer. Red circle shows the hole after sample collection.

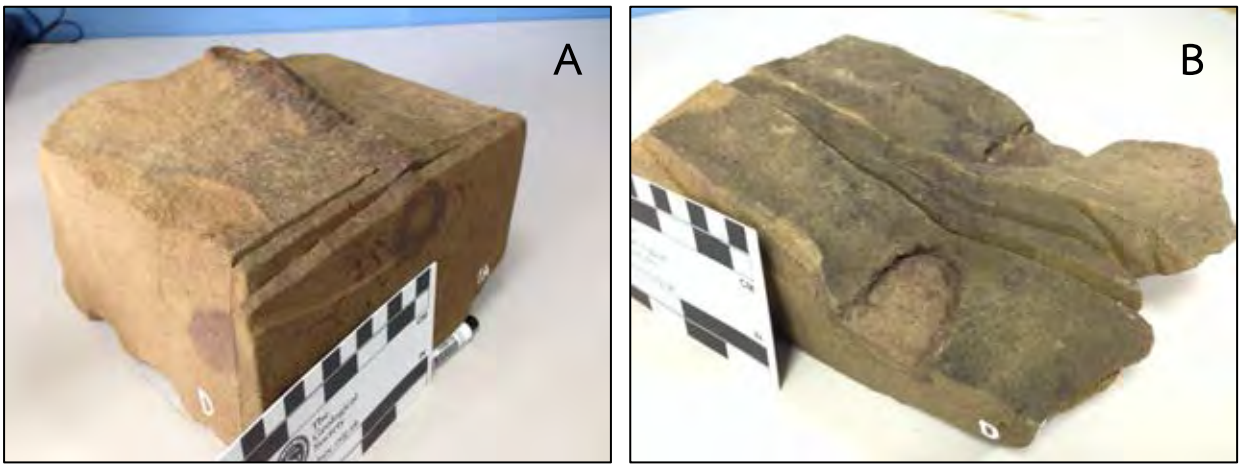

Figure 2.3 Two specimens were collected by automatic chainsaw. (A) Sample A shows epirelief preservation (*Ophiomorpha nodosa* is more resistant than surrounding rock) (B) Sample B shows hyporelief preservation (*Ophiomorpha nodosa* is less resistant than surrounding rock).

2.2 Samples preparation

2.2.1 Rock slabs

We cut samples into slabs (7x15x1 cm.) by using saw blades (lubricated by water) along cross-section of *Ophiomorpha nodosa* (see on figure 2.6). This size of slab can be put in Itrax XRF core scanner in order to measure elemental contents.

Figure 2.4 Saw blades.

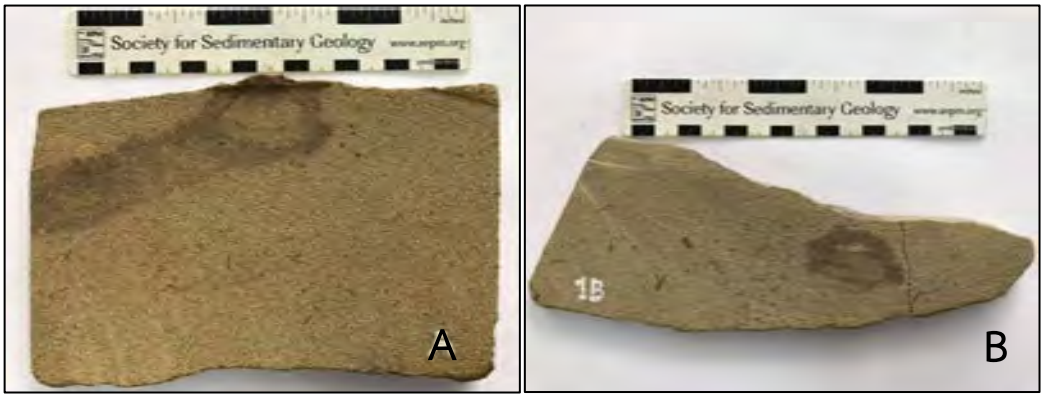

Figure 2.5 Cross-section of *Ophiomorpha* (A) Epirelief sample (B) Hyporelief sample.

Figure 2.6 Itrax XRF core scanner (https://twitter.com/geographyuom).

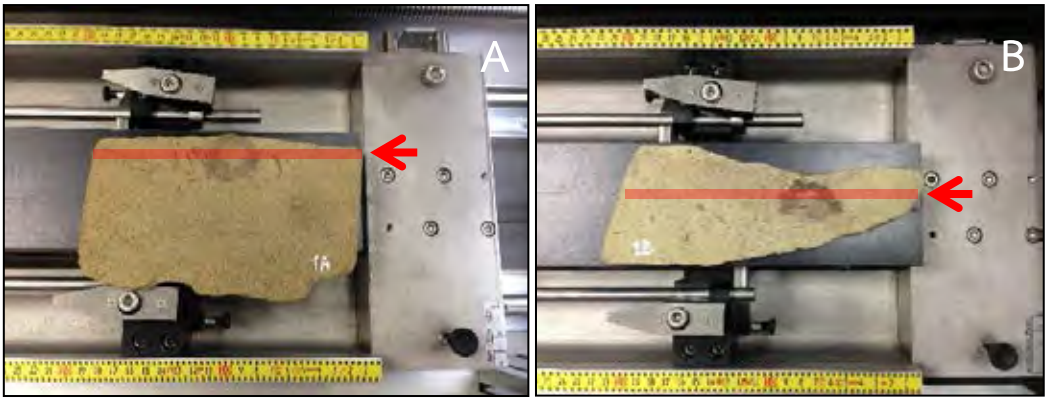

Figure 2.7 Itrax XRF measures on the red line (A) Epirelief sample (B) Hyporelief sample.

2.2.2 Thin-section

Thin-sections were prepared for both area in the trace fossil *Ophiomorpha nodosa* and in surrounding rock to observe mineralogy under microscope. First, the slabs with proper sized were attached to the glass using glue (Glue A: B: Alcohols; 1:4:1). Then using vacuum pump for sticking the glues into prepared sample, after that let the prepared sample dry for 1 day. Second, start grinding one side of the prepared sample to remove the glues surface (Fig. 2.8) then Stick the glass slide on this side with special glue, after that let them dry and stick for 1 day. Third, start grinding on other side to make it thin enough to see under microscope and then use the diamond sand for finer grinding (Fig. 2.9). Next using a special glue to stick cover glass on the thin-section. Finally, thin-section is ready for seeing mineralogy under microscope.

Figure 2.8 Coarse grinding machine.

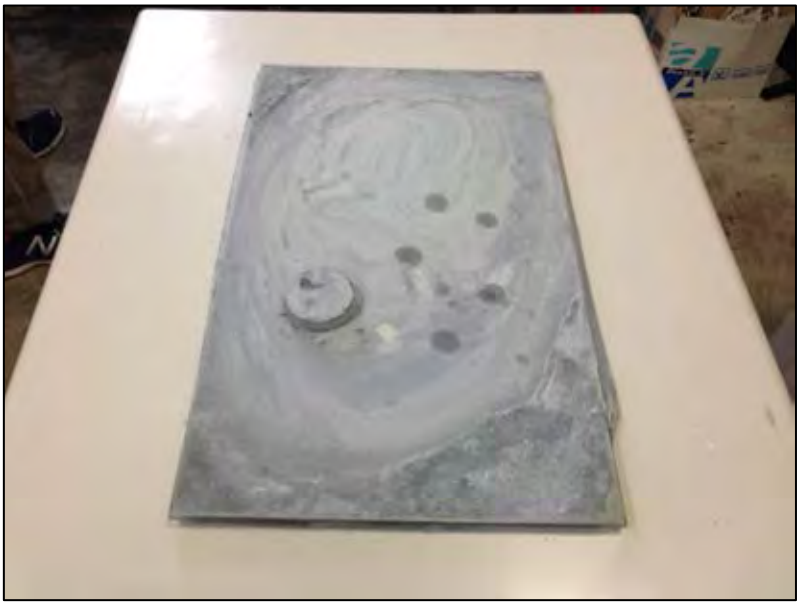

Figure 2.9 Diamond sand.

Figure 2.10 (A) Glue A is Epoxy hardener (B) Glue B is Epoxy resin.

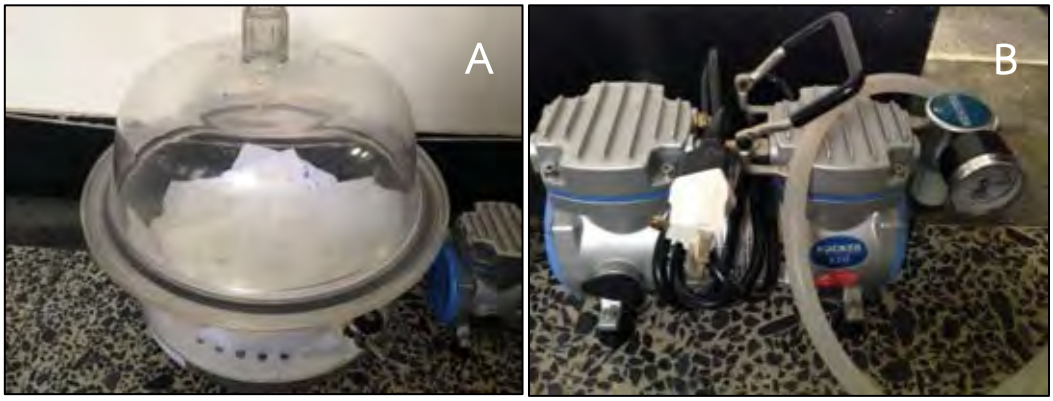

Figure 2.11 (A) Vacuum pot (B) Pumping machine.

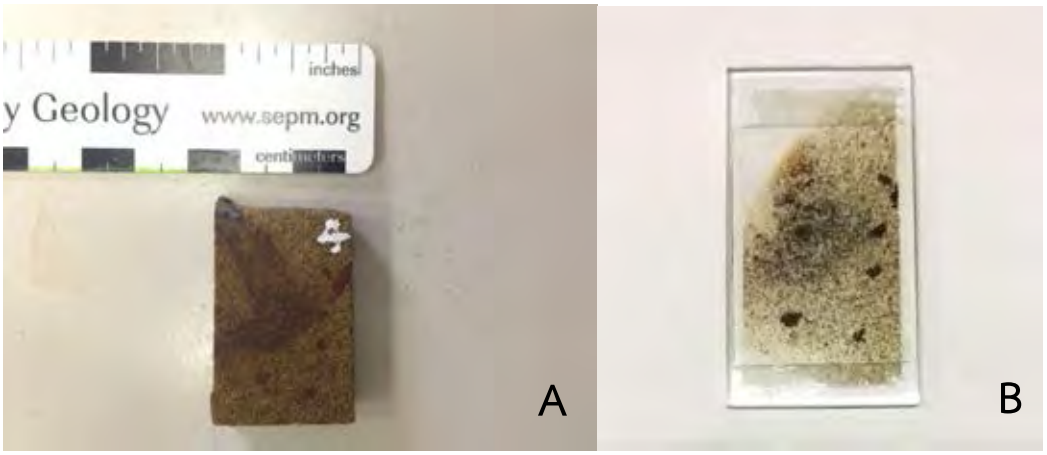

Figure 2.12 (A) Selected sample uses for doing thin-section (B) Completed thin-section slide.

Figure 2.13 Microscope.

2.2.3 Sample preparation for XRD and XRF

After we finish Itrax XRF measurement, we used the same slabs and focus on the trace fossil *Ophiomorpha nodosa* by using rasp to sharpen only *Ophiomorpha nodosa* pieces (Fig. 2.14) and then crush these pieces into powder for measure water content, X-ray diffractometer (XRD) and Wavelength Dispersive X-ray fluorescence (WD-XRF) analysis in order to compare chemical composition with Itrax XRF data. We also measure chemical composition of the inside and surrounding rock with the same methods.

For XRD analysis, we crush *Ophiomorpha nodosa* pieces (Fig. 2.14) to prepare sample into powder by using vibratory disc mill. The powder samples were put in pellet plates (Fig.2.17) for measuring XRD analysis by using X-ray Diffractometer (XRD-Bruker model D8 advance). For XRF analysis, the powder samples were weighed 8 grams and mix with flux powder 1 grams and pack on plates using compressor (Fig.2.18)

for measuring XRF analysis with Wavelength Dispersive X- ray Fluorescence Spectrometer (WD-XRF, brand of Bruker model S4 pioneer).

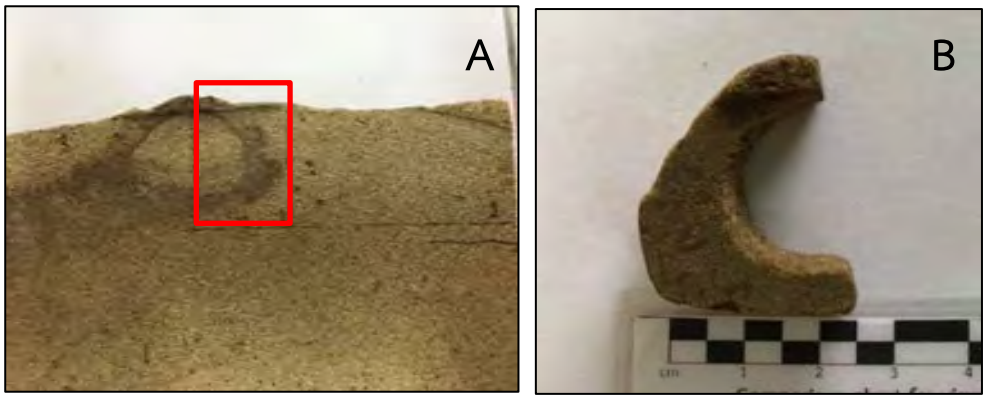

Figure 2.14 (A) Focus on the trace fossil *Ophiomorpha nodosa* on red square (B) Shapened *Ophiomorpha nodosa* piece.

Figure 2.15 Powder samples prepare to steam in oven with 105° celcius to measure water content.

Figure 2.16 Sample compressor for XRF analysis.

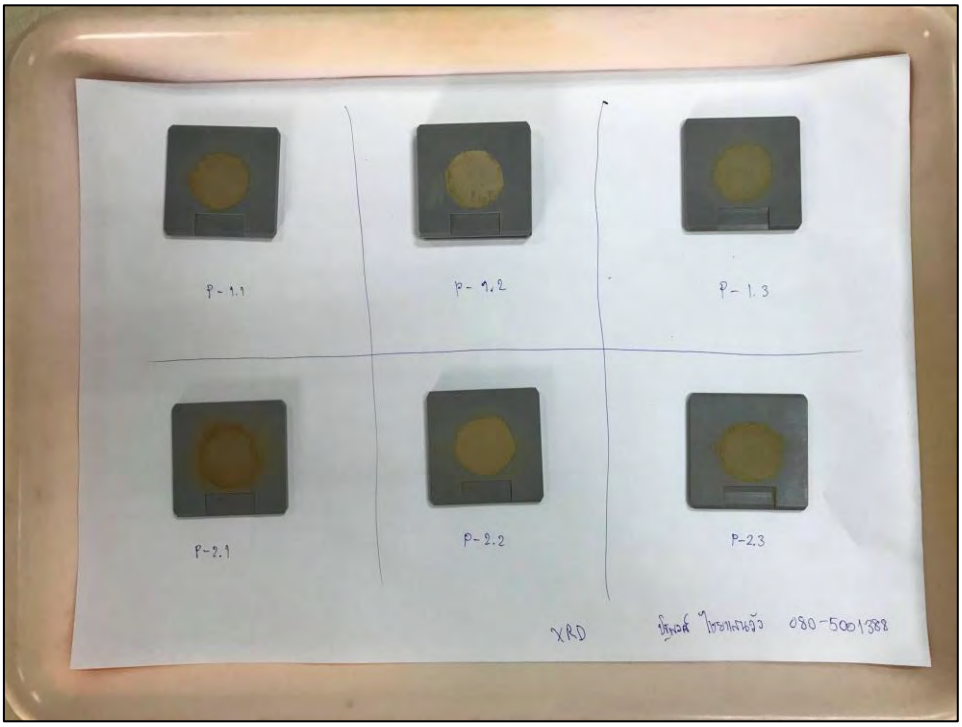

Figure 2.17 Sample packing for XRD analysis.

Figure 2.18 Sample packing for XRF analysis.

2.3 Data processing

2.3.1 ITRAX XRF core scanning

The XRF scanning elemental data displays in count per seconds per unit time and unit scale (cps). The data for sample A were smoothed to 200 microns of step size using a ten-point average. The graphs were plotted by using Grapher10 program. Main elements were selected to display results (i.e. Si, Al, Fe, K, Ca). Also, raw data (non-average) were plotted to see trends of graph peak compare to average data.

2.3.2 X-Ray Diffraction (XRD)

After running all samples, we use program named "EVA" to determining results. First, we import files of sample analysis from XRD Commander that runs analyzing samples. Then open files smooth graph of XRD and next append "Background" by selecting on "Enhanced", adjust to minimum (Curvature = 0). Determine only Enhanced background file to identify mineralogy comparing to the library data.

In this study, we also use MAUD program by importing files from XRD commander. It can be used for identify mineral and determining weight percentage of mineral in quantitative analysis.

2.3.3 X-Ray Fluorescence (XRF)

After running all samples, we use program named “Spectra Plus Launcher” on evaluation. Select all samples display on interactive quantitative mode. First, we have to add data of samples’ weight and flux powder’s weight in “Sample properties”. After that we can see amount of element in oxide and also view peak of elements’ graph by using mode “View scan” on column of “Line 1 of oxide elements”. We consider graph that show peak (on the red line) of Oxide elements, the red line peak should be center on the peak. If it is not, they will be ignored on this Oxide elements (It infers that element is too few or no detection amount). Finally, using “Normalize” and export to Excel.

2.3.4 Thin-section

Thin-section’s samples are determined under polarized-light microscope. We can use “NIS-elements BR” program for counting grains of mineral, observing grain size, compaction, matrix contribution, mineralogy and petrography. The point counting method can infer amount of grains of mineral. This can be used to identify the name of rock.

Chapter 3

Results

3.1 ITRAX X-Ray Fluorescence (XRF) data

3.1.1 The ratio of main elements

For ITRAX core scanning XRF data. Firstly, main elements were selected based on the number of count per sec (cps). Then ratio of each element is calculated by dividing with total count per second. Some elements were ignored with little concentration.

Each sample A was scanned two times. On sample A, it was also scanned in 2 directions (Fig. 3.1).

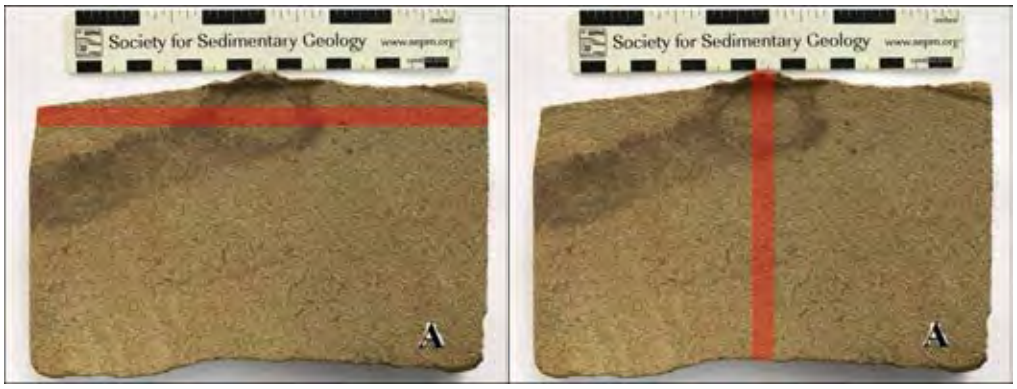

Figure 3.1 Scanning line displays on thin slab of sample A (Left) First scan in named "Ophio_1A_R1". (Right) Second scan in named "Ophio_1A_Bottom"

➢ Sample A (Ophio_1A_R1)

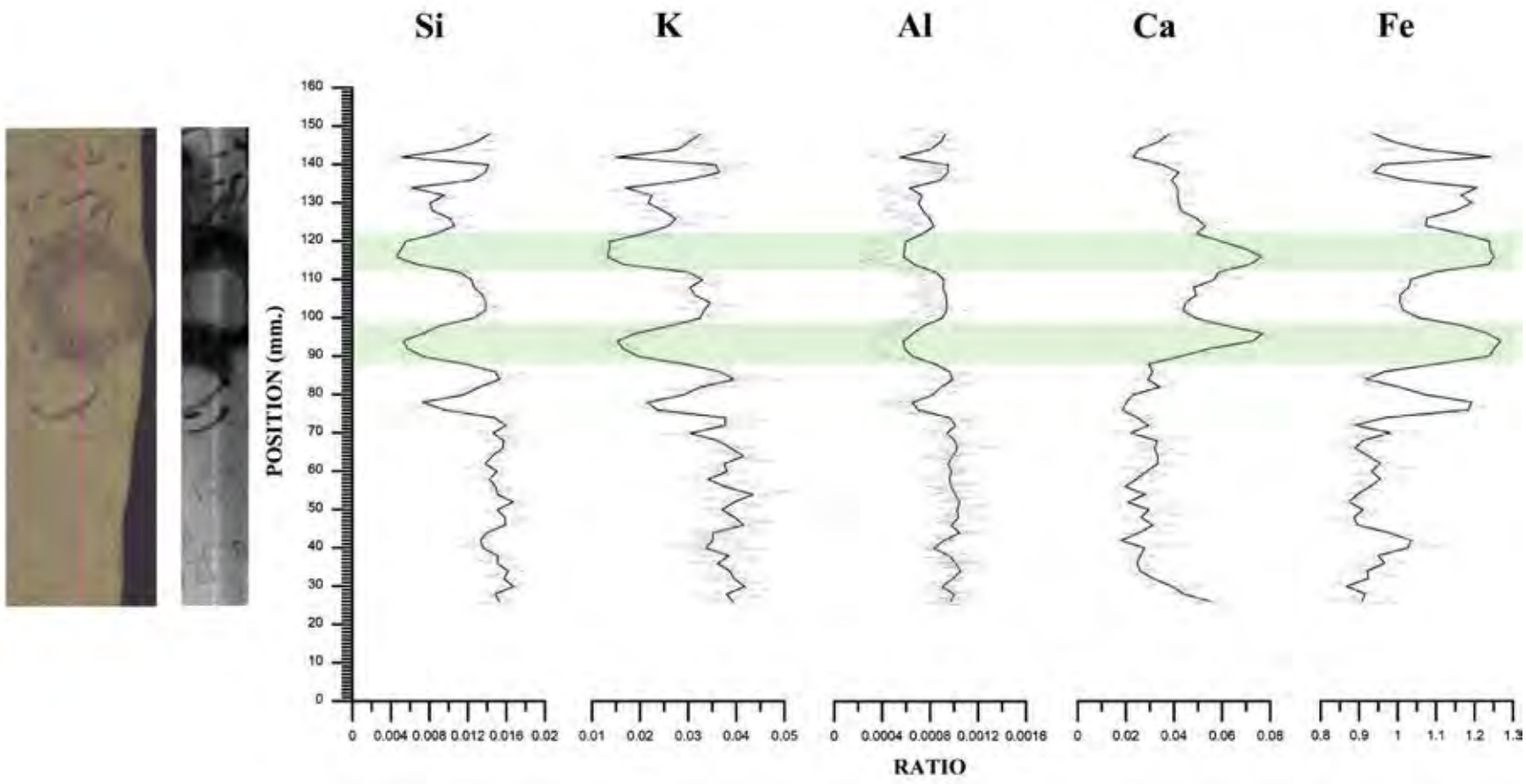

Figure 3.2 Graph data of ITRAX XRF core scanning displays main elements in ratio and position compare with optical and radiograph images. The pink line on optical image is the scanning line. The blue line displays peak of graph data where *Ophiomorpha nodosa* is located.

➢ Sample A (Ophio_1A_Bottom)

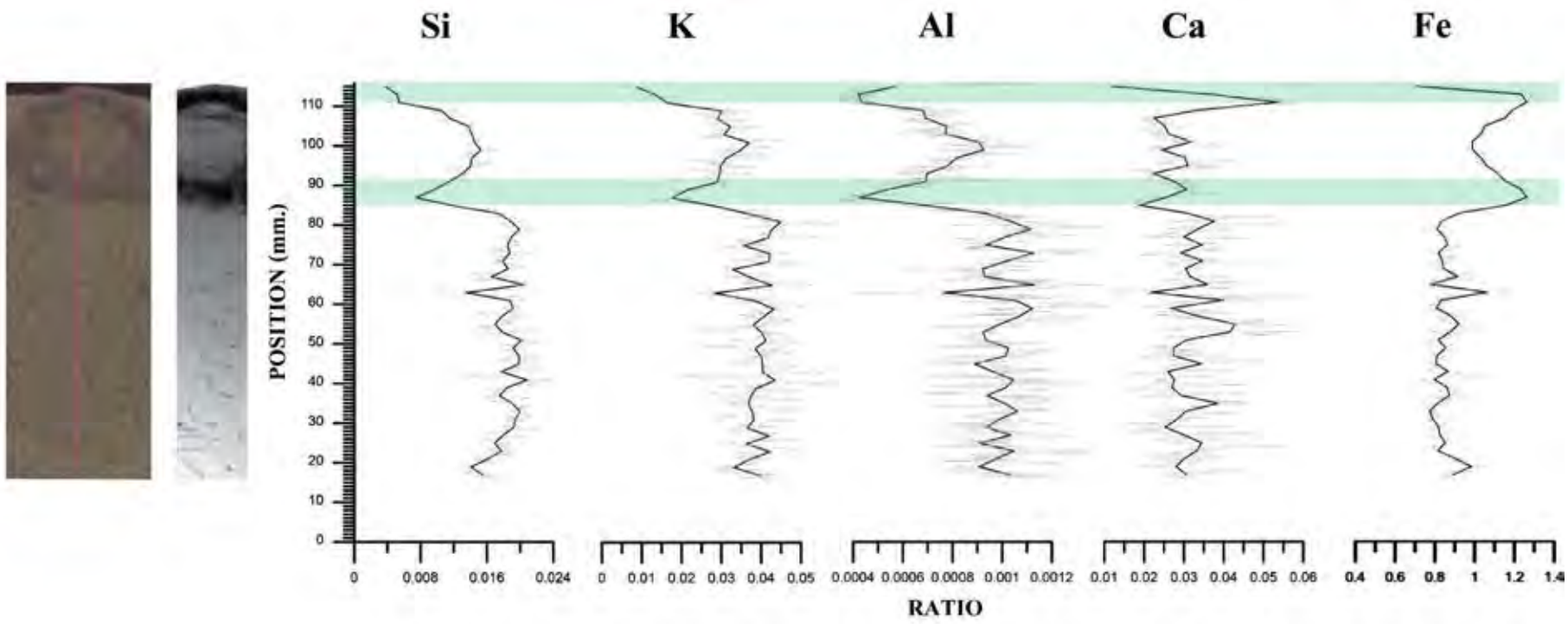

Figure 3.3 Graph data of ITRAX XRF core scanning displays main elements in ratio and position compare with optical and radiograph images. The pink line in optical image is the scanning line. The blue line displays peak of graph data where *Ophiomorpha nodosa* is located.

Also, sample B is scanned with two times but same direction by the first one focus only part of *Ophiomorpha nodosa* and second one is longer scanned. (Fig.3.4)

Figure 3.4 Scanning line displays on thin slab of sample B (Left) First scan in named "Ophio_1B_R1". (Right) Second scan in named "Ophio_1B_R2"

➢ Sample B (Ophio_1B_R1)

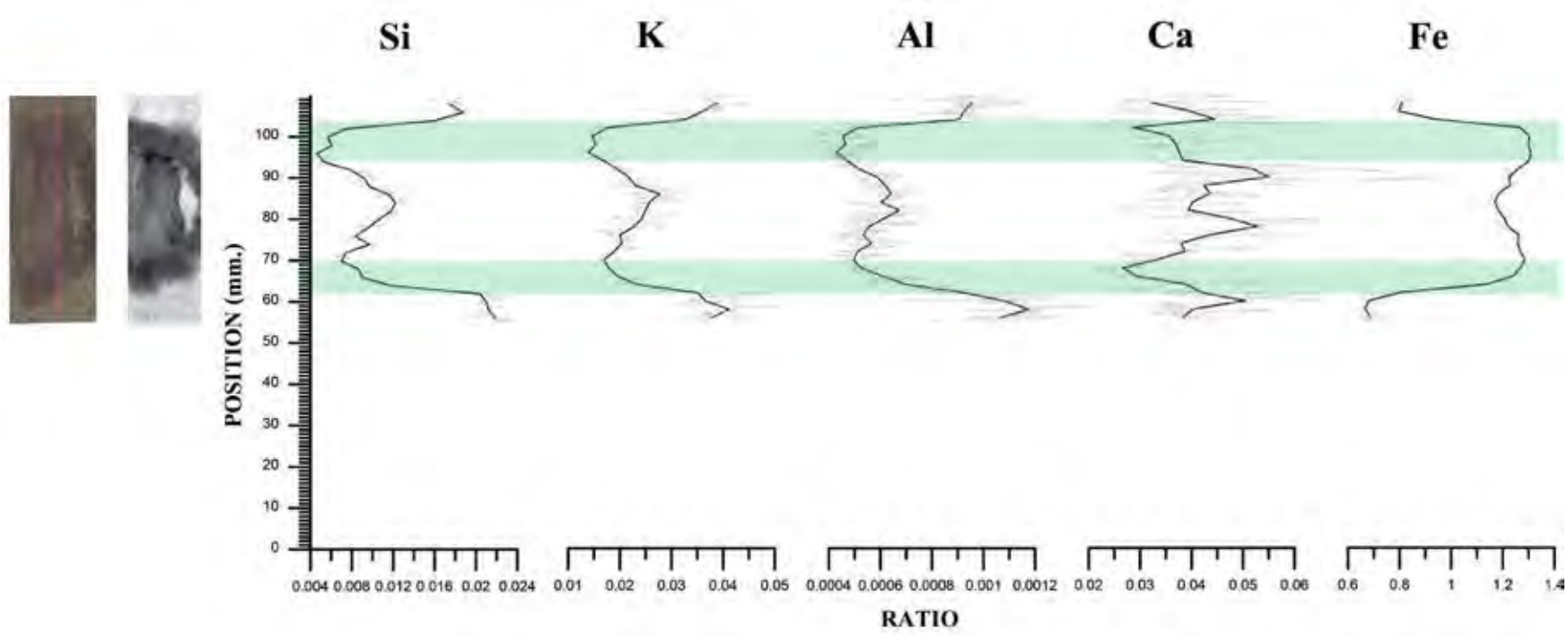

Figure 3.5 Graph data of ITRAX XRF core scanning displays main elements in ratio and position compare with optical and radiograph images. The pink line in optical image is the scanning line. The blue line displays peak of graph data where *Ophiomorpha nodosa* is located.

➢ Sample B (Ophio_1B_R2)

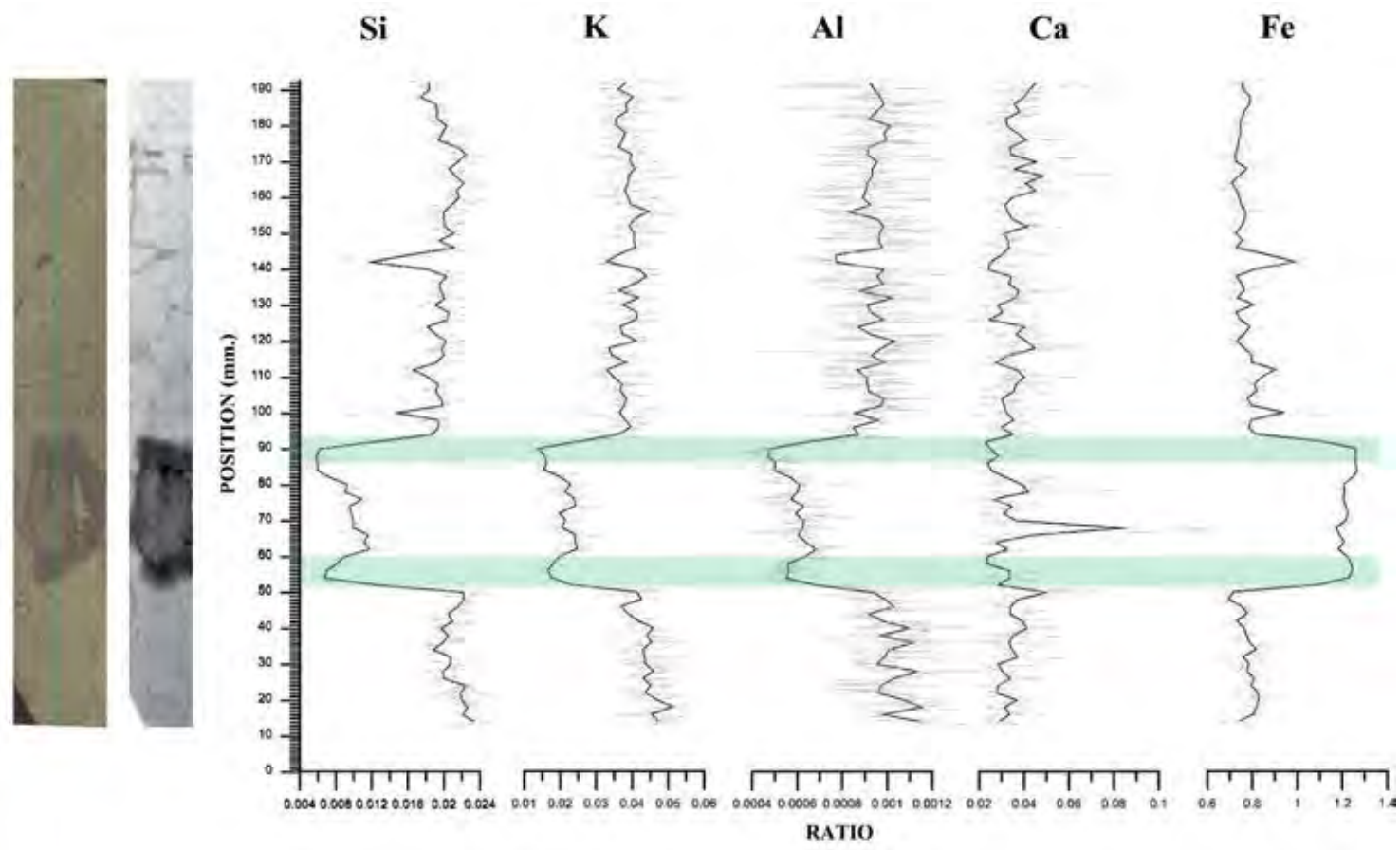

Figure 3.6 Graph data of ITRAX XRF core scanning displays main elements in ratio and position compare with optical and radiograph images. The pink line in optical image is the scanning line. The blue line displays peak of graph data where *Ophiomorpha nodosa* is located.

3.1.2 Elemental correlation

Correlation coefficient is used for observing relationship of individual elements. Table 1 and Table 2 show the ITRAX XRF elemental data, the correlation coefficient for each pair of element variables, positively correlated variable (r>0), and negatively correlated variable (r<0). The red color shows the r values more than 0.700 and the yellow color shows the r values less than -0.700.

Sample A (Ophio_1A_R1)

	Si	Al	Fe	K	Ca
Si					
Al	0.974				
Fe	-0.977	-0.961			
K	0.974	0.956	-0.966		
Ca	-0.59	-0.549	0.564	-0.576	

Table 1 Correlation coefficient of sample A (Ophio_1A_R1)

Sample A (Ophio_Bottom)

	Si	Al	Fe	K	Ca
Si					
Al	0.924				
Fe	-0.769	-0.830			
K	0.941	0.935	-0.684		
Ca	0.150	0.123	0.010	0.197	

Table 2 Correlation coefficient of sample A (Ophio_Bottom)

Also, sample B is correlated to show on Table 3 and Table 4 of correlation coefficient of sample B (Ophio_1B_R1) and sample B (Ophio_1B_R2) respectively.

Sample B (Ophio_1B_R1)

	Si	Al	Fe	K	Ca
Si					
Al	0.979				
Fe	-0.976	-0.984			
K	0.976	0.97	-0.96		
Ca	0.171	0.144	-0.132	0.205	

Table 3 Correlation coefficient of sample B (Ophio_1B_R1)

Sample B (Ophio_1B_R1)

	Si	Al	Fe	K	Ca
Si					
Al	0.933				
Fe	-0.967	-0.924			
K	0.944	0.95	-0.919		
Ca	0.145	0.119	-0.163	0.074	

Table 4 Correlation coefficient of sample B (Ophio_1B_R2)

3.1.3 Principle component analysis (PCA)

Principle component analysis is also used in order to explain the relationship of each elements by plotting on mono plot graph. Vectors display pointing away from the origin to represent the original variables. The angle between vectors is the correlation between other elements, a small angle indicates the variables are positively correlated, an angle of 90° indicates the variables are not correlated, and angle of 180° indicates the variables are negatively correlated. The closeness to the circle of each vectors indicated how well of each element is represented in the plot.

On Figure 3.7 shows two mono plot graphs of sample A. Main elements are correlated show that Silicon (Si), Potassium (K) and Aluminium (Al) have negative relationship with Iron (Fe).

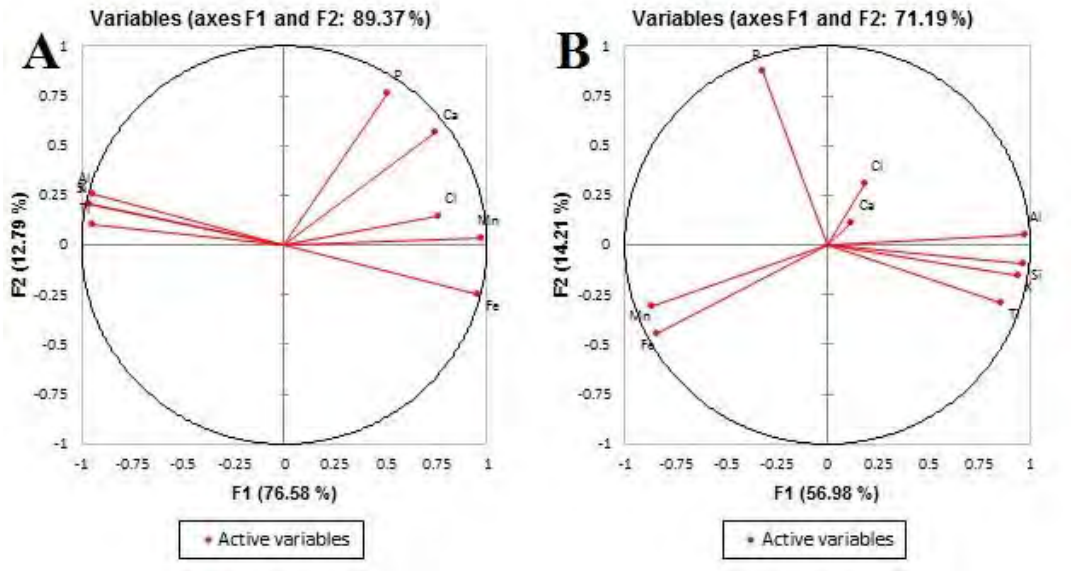

Figure 3.7 (A) Principle component of sample A (Ophio_1A_R1) (B) Principle component of sample A (Ophio_1A_Bottom)

On Figure 3.8 shows two mono plot graphs of sample B. Main elements are correlated. There is the same relationship compare with mono plot of sample A. However, there is only Calcium (Ca) has no relationship with another.

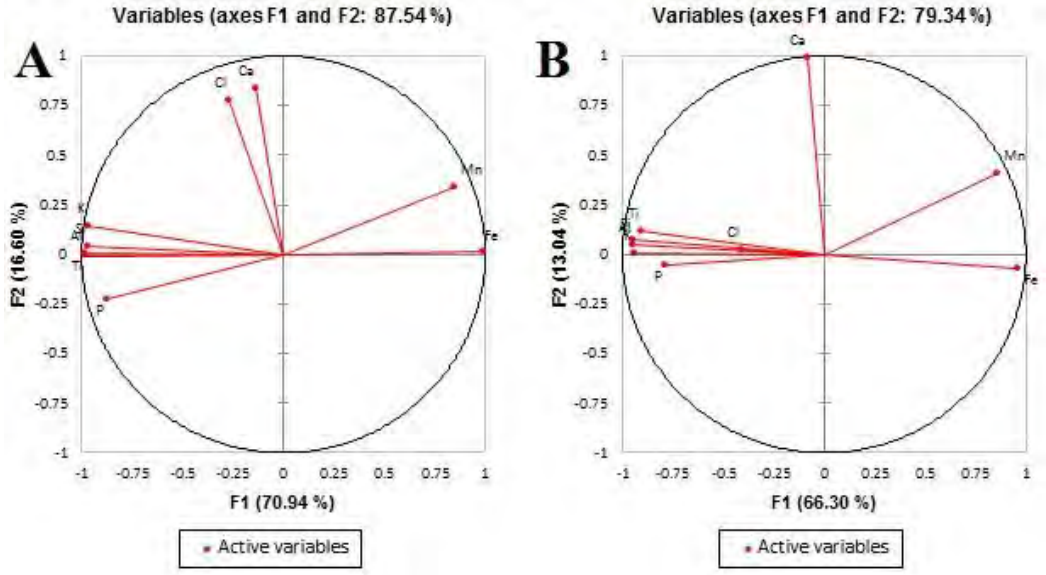

Figure 3.8 (A) Principle component of sample B (Ophio_1B_R1) (B) Principle component of sample B (Ophio_1B_R2)

3.2 X-Ray Fluorescence (XRF) Data

3.2.1 Calibration curve of standard oxide elements

➢ Sample A

Formula	Concentration (%wt)		
	Ophiomorpha nodosa	Burrow fill	Host rock
SiO_2	47.18	62.88	64.69
Fe_2O_3	27.21	16.22	10.71
Al_2O_3	10.09	9.76	12.22
CaO	3.30	1.80	1.72
MgO	3.11	2.09	2.99
K_2O	2.65	3.49	3.58
Na_2O	1.57	1.41	1.82
Water content	2.5	2.1	1.4
	97.61	99.75	99.14

Table 5 Concentration (%wt) of XRF data of sample A

➢ Sample B

Formula	Concentration (%wt)		
	Ophiomorpha nodosa	Burrow fill	Host rock
SiO_2	51.13	70.12	66.90
Fe_2O_3	23.09	6.33	8.45
Al_2O_3	12.57	12.92	12.88
CaO	2.95	1.48	1.82
MgO	3.74	3.67	2.80
K_2O	2.70	2.19	3.52
Na_2O	1.44	2.13	1.78
Water content	3.0	0.1	1.8
	99.63	98.94	99.94

Table 6 Concentration (%wt) of XRF data of sample B

3.3 X-Ray Diffraction (XRD) Data

3.3.1 Sample A

- *Ophiomorpha nodosa*

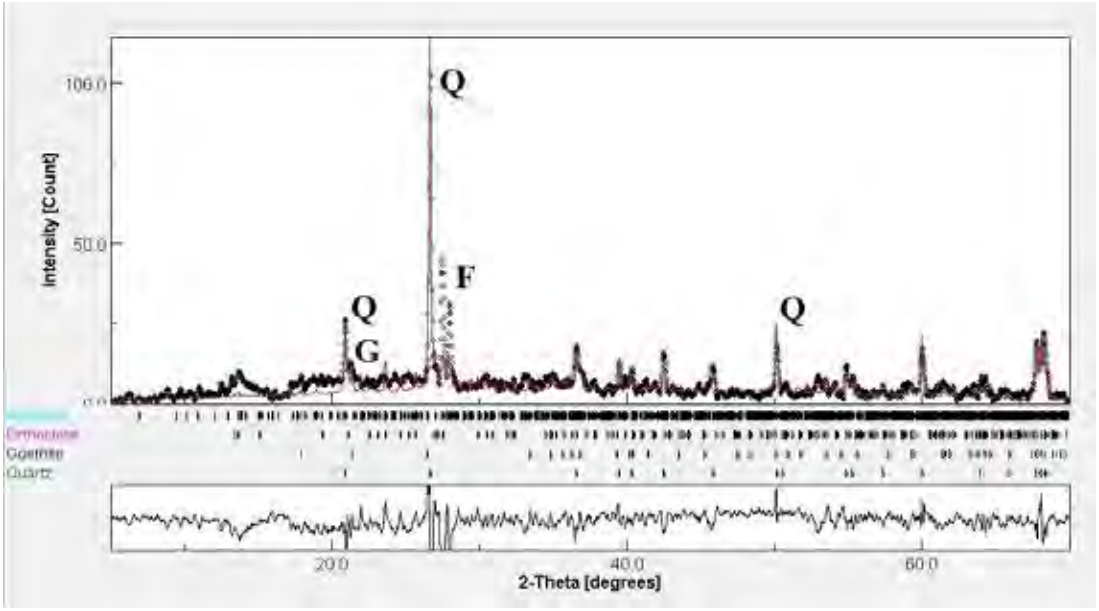

Figure 3.9 Graph XRD data of *Ophiomorpha nodosa* of sample A (Q=Quartz, F=Feldspar, G=Goethite)

Mineral	Amount (%wt)	Error
Quartz	44.97	±0.00
Anorthite	28.41	±2.15
Orthoclase	21.16	±1.66
Goethite	5.45	±0.45
	99.99	

Table 7 Mineral content of *Ophiomorpha nodosa* of sample A

➢ Burrow fill

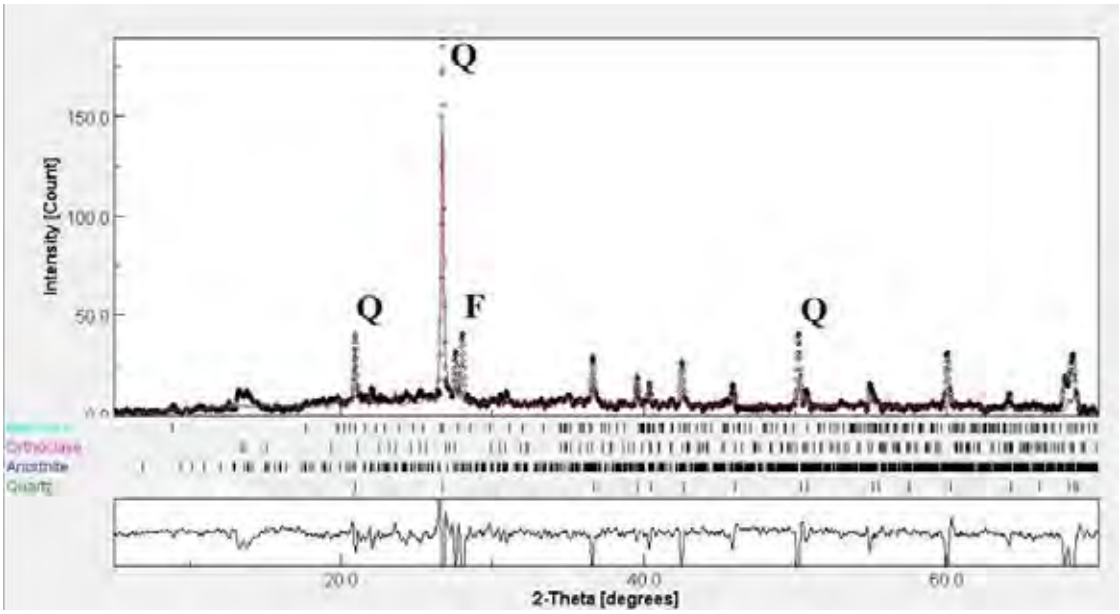

Figure 3.10 Graph XRD data of burrow fill of sample A (Q=Quartz, F=Feldspar)

Mineral	Amount (weight %)	Error
Quartz	61.62	±0.00
Orthoclase	14.27	±1.60
Anorthite	14.11	±1.77
Illite-mica	10.00	±1.67
	100.00	

Table 8 Mineral content of burrow fill of sample A

➢ Host rock

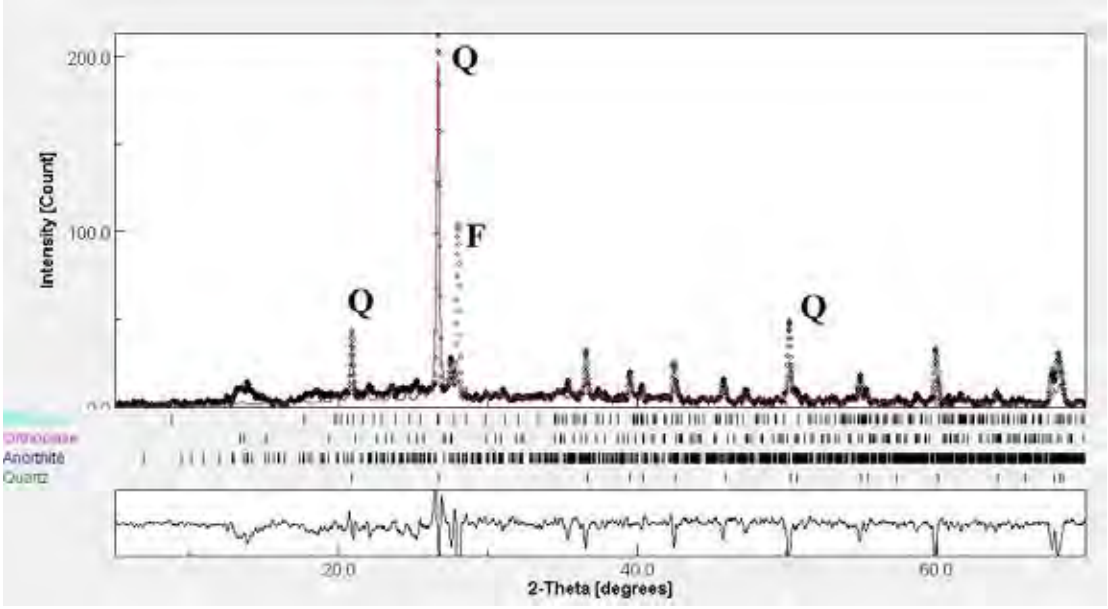

Figure 3.11 Graph XRD data of substrate of sample A (Q=Quartz, F=Feldspar)

Mineral	Amount (%wt)	Error
Quartz	57.00	±0.00
Anorthite	21.29	±1.63
Illite-mica	13.39	±1.34
Orthoclase	8.32	±1.22
	100.00	

Table 9 Mineral content of host rock of sample A

3.3.2 Sample B

➢ *Ophiomorpha nodosa*

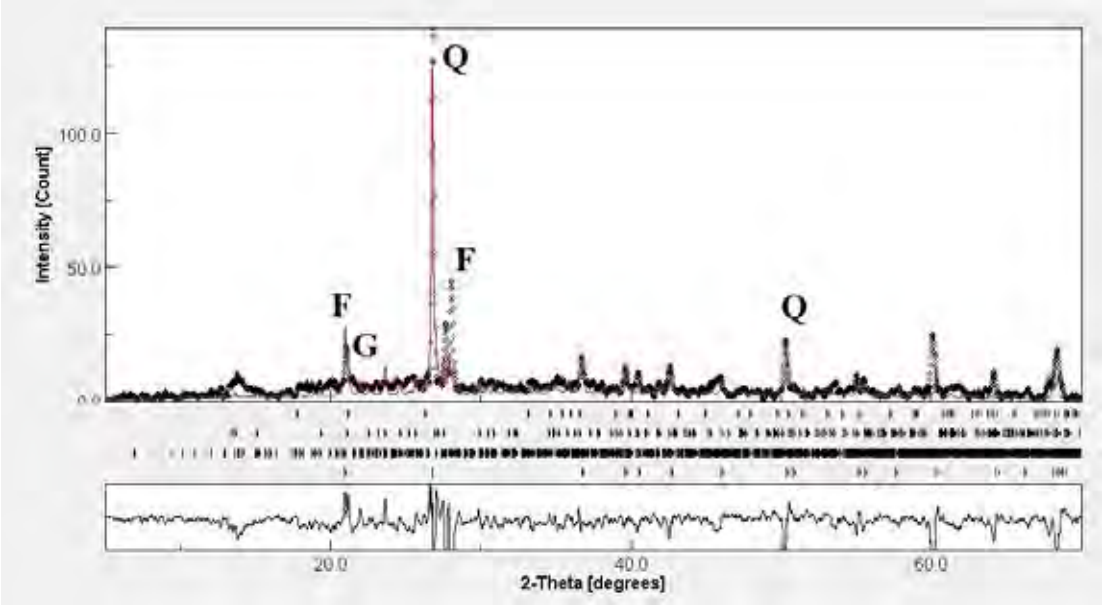

Figure 3.12 Graph XRD data of *Ophiomorpha nodosa* of sample B (Q=Quartz, F=Feldspar, G=Goethite)

Mineral	Amount (%wt)	Error
Quartz	50.65	±0.00
Anorthite	22.44	±2.07
Orthoclase	20.81	±1.79
Goethite	6.10	±0.66
	100.00	

Table 10 Mineral content of *Ophiomorpha nodosa* of sample B

➢ Burrow fill

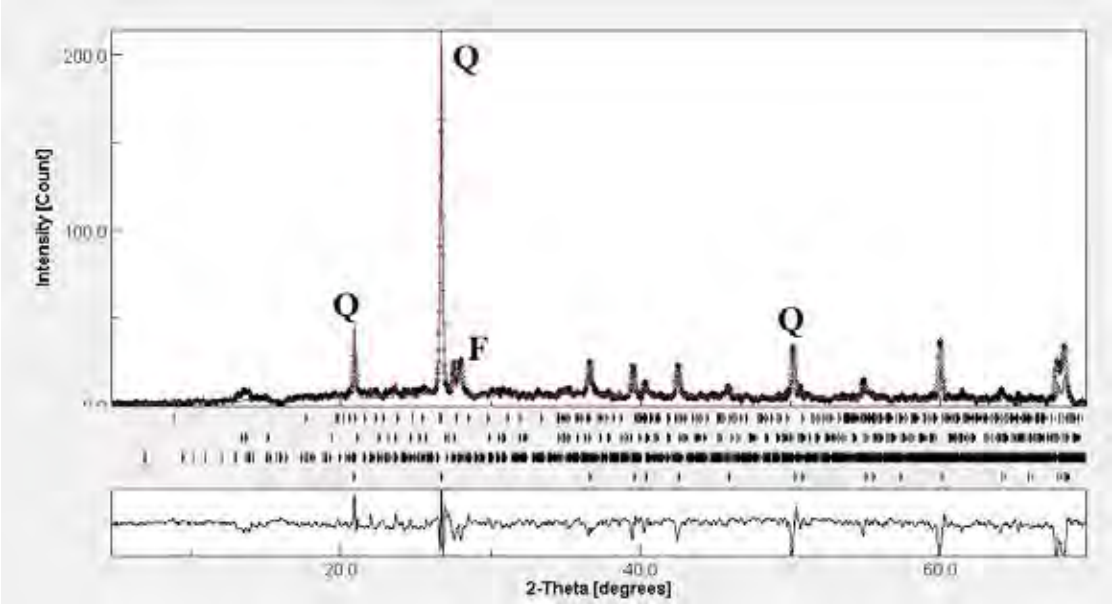

Figure 3.13 Graph XRD data of burrow fill of sample B (Q=Quartz, F=Feldspar)

Mineral	Amount (%wt)	Error
Quartz	63.50	±0.00
Anorthite	19.51	±1.45
Orthoclase	8.82	±1.06
Illite-mica	8.17	±1.18
	100.00	

Table 11 Mineral content of burrow fill of sample B

➢ Host rock

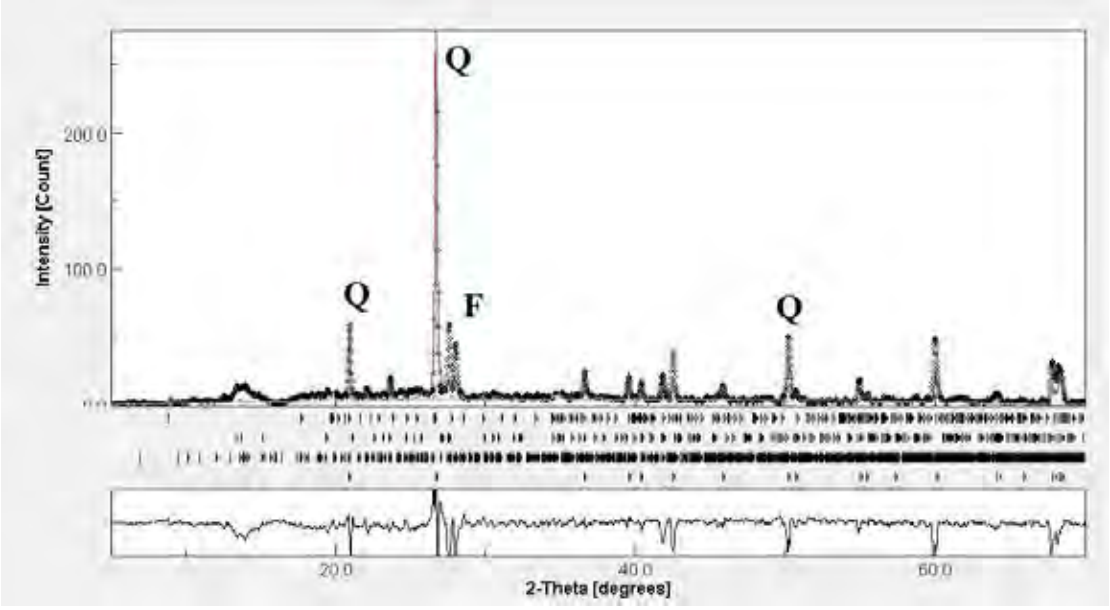

Figure 3.14 Graph XRD data of host rock of sample B (Q=Quartz, F=Feldspar)

Mineral	Amount (%wt)	Error
Quartz	62.14	±0.00
Anorthite	17.74	±1.42
Illite-mica	10.47	±1.25
Orthoclase	9.65	±1.06
	100.00	

Table 12 Mineral content of host rock of sample A

3.4 Petrography

3.4.1 Sample A

In thin-section method, we select part of both the presence of *Ophiomorpha nodosa* and substrate of surrounding rock in order to observe petrography of the whole rock (Fig. 3.15). We also observe burrow fill inside *Ophiomorpha nodosa* to compare petrography with surrounding rock.

Figure 3.15 (Left) *Ophiomorpha nodosa*-dominated rock (from sample A) using for prepare thin-section (Right) Thin-section of sample A

➢ *Ophiomorpha nodosa*

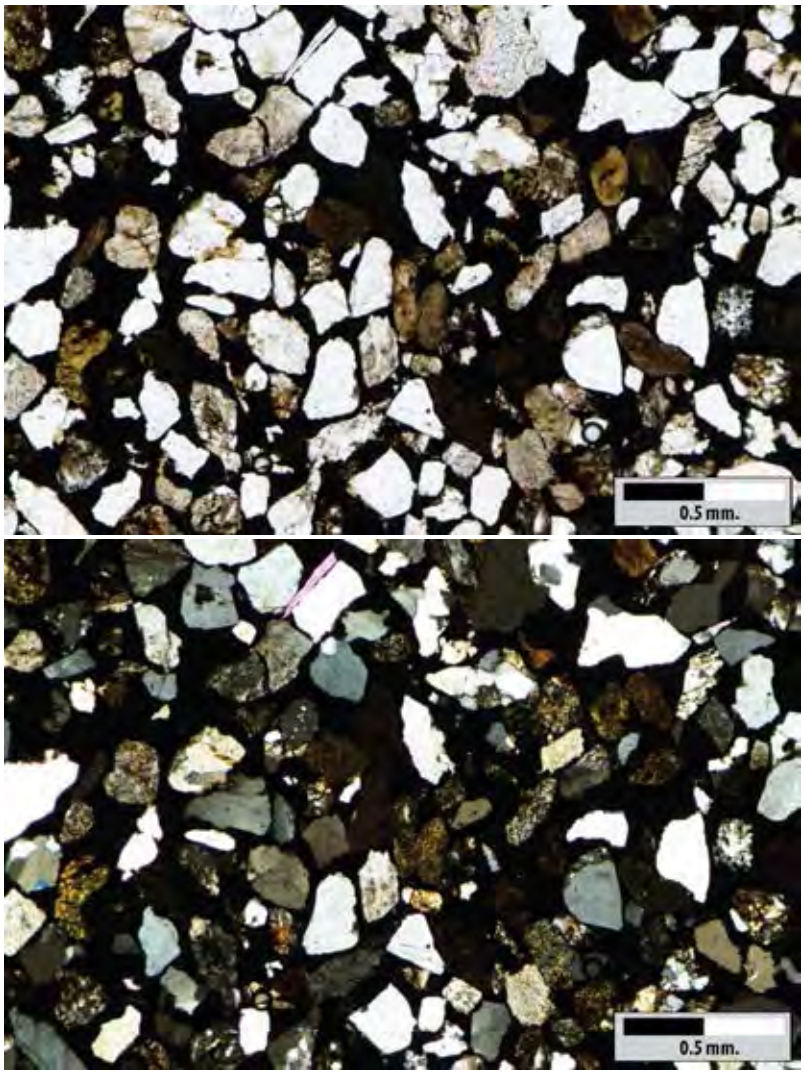

Figure 3.16 Thin-section of sample A at *Ophiomorpha nodosa* (Top) PPL (Bottom) XPL (5X)

Mineral	Amount	
Quartz	95	0.55
Rock fragment	59	0.34
Feldspar	20	0.11
	174	1.00

Table 13 Amount of minerals in thin-section of sample A at *Ophiomorpha nodosa*

➢ Burrow Fill

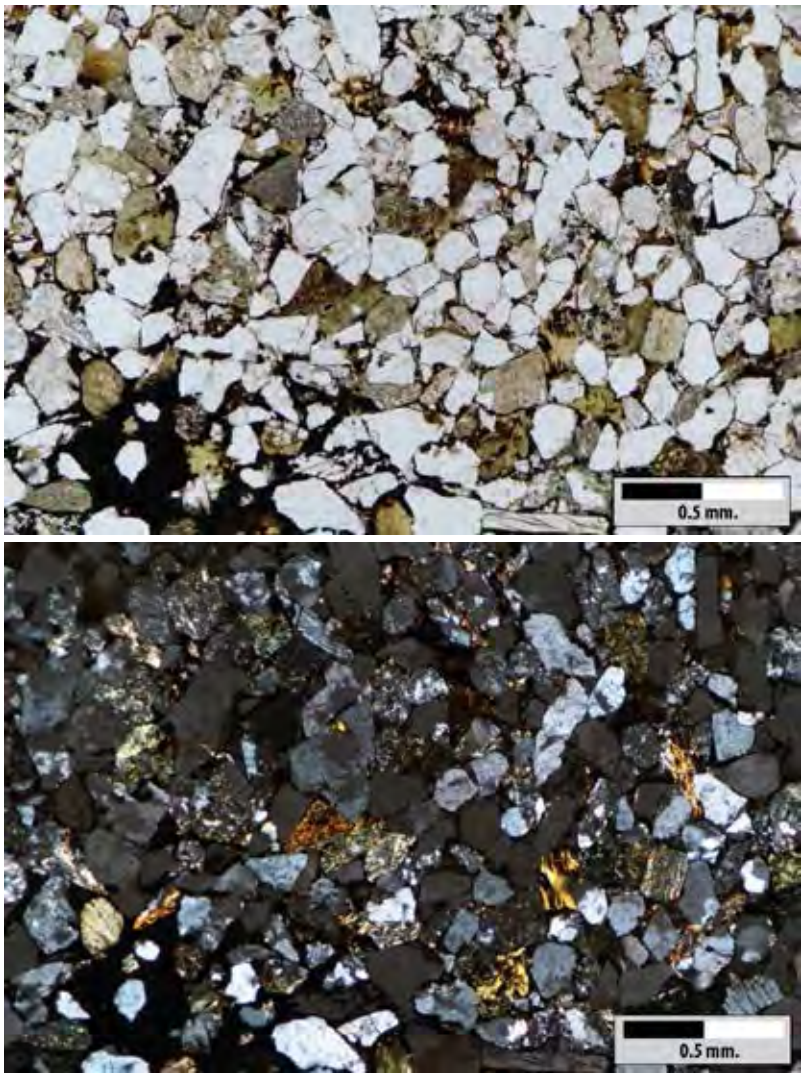

Figure 3.17 Thin-section of sample A at burrow fill (Top) PPL (Bottom) XPL (5X)

Mineral	Amount	
Quartz	95	0.47
Rock fragment	65	0.32
Feldspar	39	0.19
Mica	3	0.02
	202	1.00

Table 14 Amount of minerals in thin-section of sample A at burrow fill.

➢ Host rock

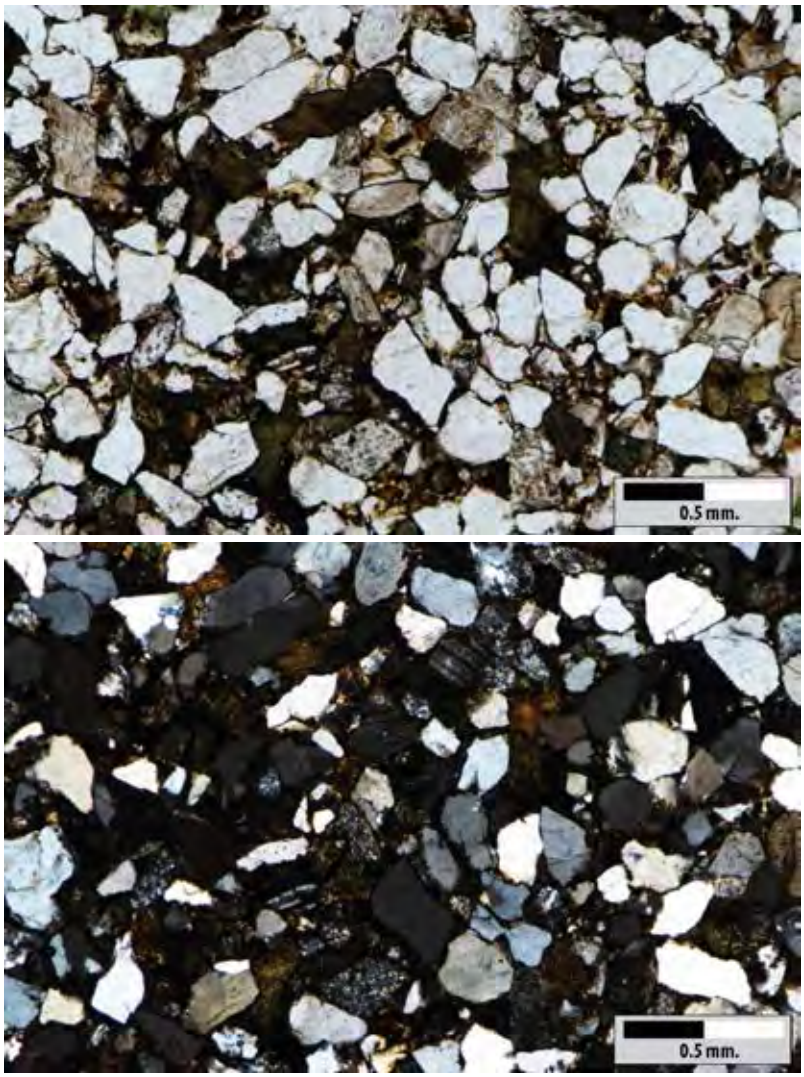

Figure 3.18 Thin-section of sample A at host rock (Top) PPL (Bottom) XPL (5X)

Mineral	Amount	
Quartz	123	0.41
Rock fragment	101	0.34
Feldspar	52	0.17
Opaque minerals	22	0.07
Mica	2	0.01
	300	1

Table 15 Amount of minerals in thin-section of sample A at host rock

3.4.2 Sample B

In thin-section method, we select part of both the presence of *Ophiomorpha nodosa* and substrate of surrounding rock in order to observe petrography of the whole rock (Fig. 3.19). We also observe on burrow fill inside *Ophiomorpha nodosa* to compare petrography with surrounding rock.

Figure 3.19 (Left) *Ophiomorpha nodosa*-dominated rock (from sample B) for preparing thin-section (Right) Thin-section of sample B

➢ *Ophiomorpha nodosa*

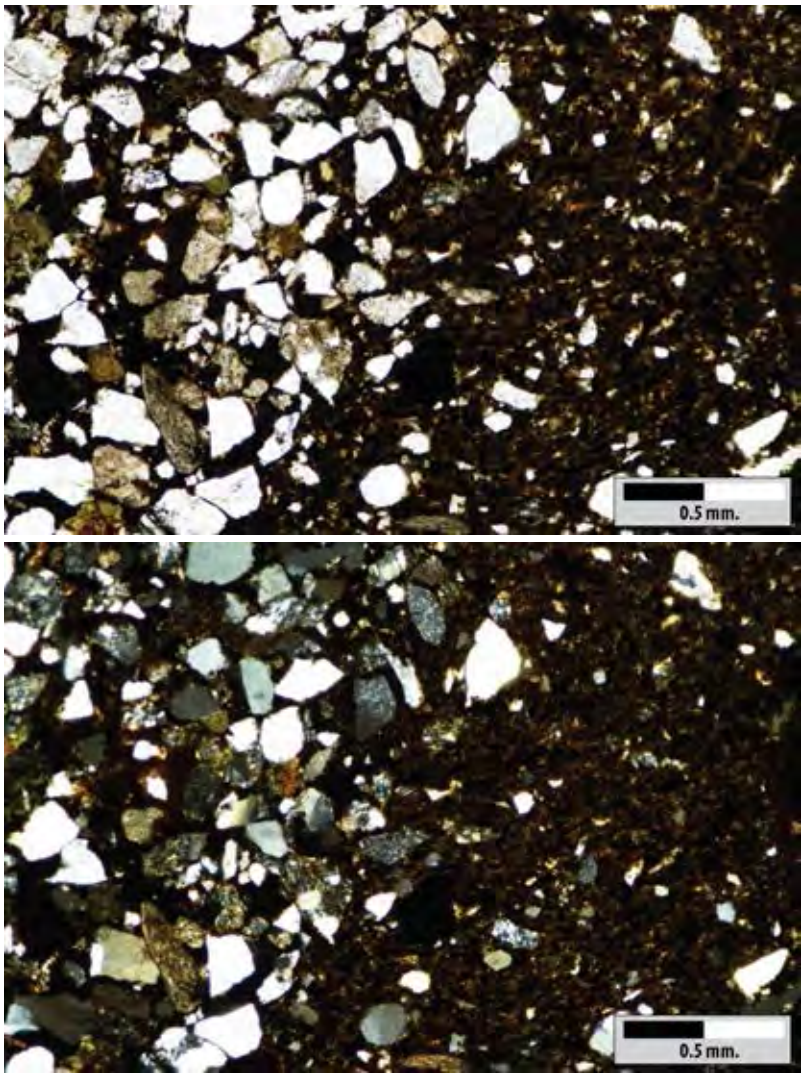

Figure 3.20 Thin-section of sample B at *Ophiomorpha nodosa* (Top) PPL (Bottom) XPL (5X)

Mineral	Amount	
Quartz	40	0.38
Feldspar	24	0.24
Rock fragment	19	0.18
Opaque minerals	17	0.16
Mica	4	0.04
	104	1

Table 16 Amount of minerals in thin-section of sample B at *Ophiomorpha nodosa*

➢ Burrow Fill

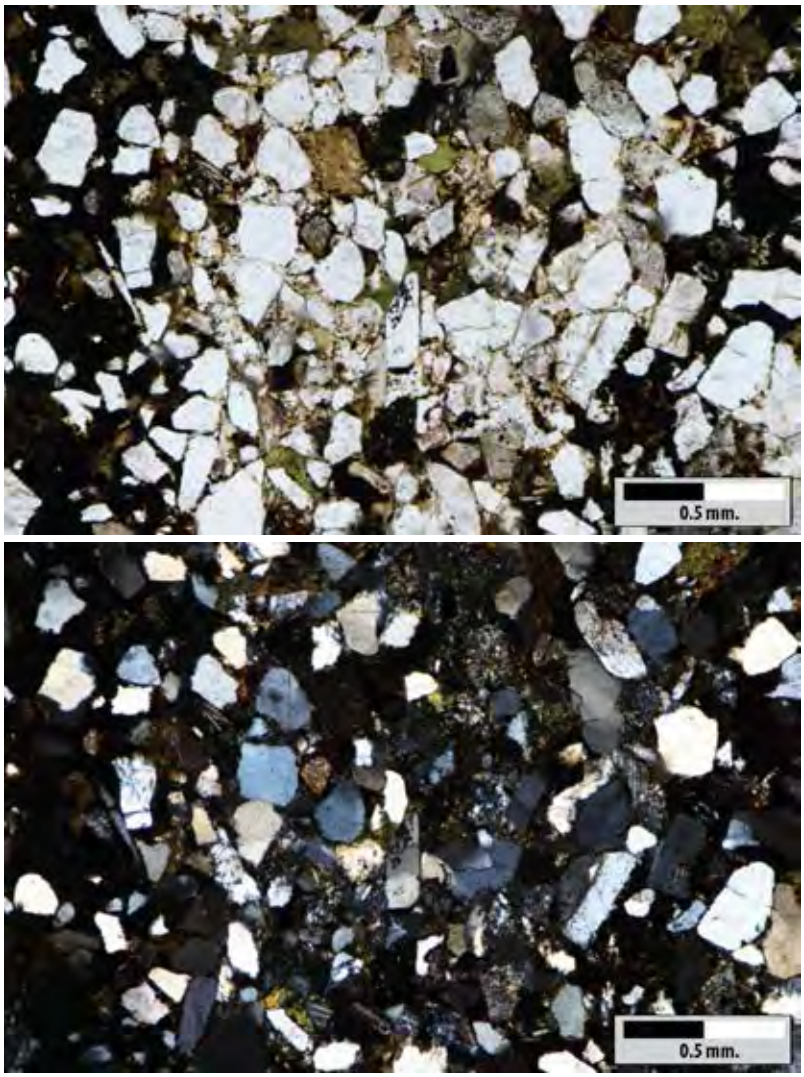

Figure 3.21 Thin-section of sample B at burrow fill (Top) PPL (Bottom) XPL (5X)

Mineral	Amount	
Quartz	122	0.49
Rock fragment	66	0.26
Feldspar	46	0.19
Opaque minerals	9	0.04
Mica	4	0.02
	247	1.00

Table 17 Amount of minerals in thin-section of sample B at burrow fill

➢ Host rock

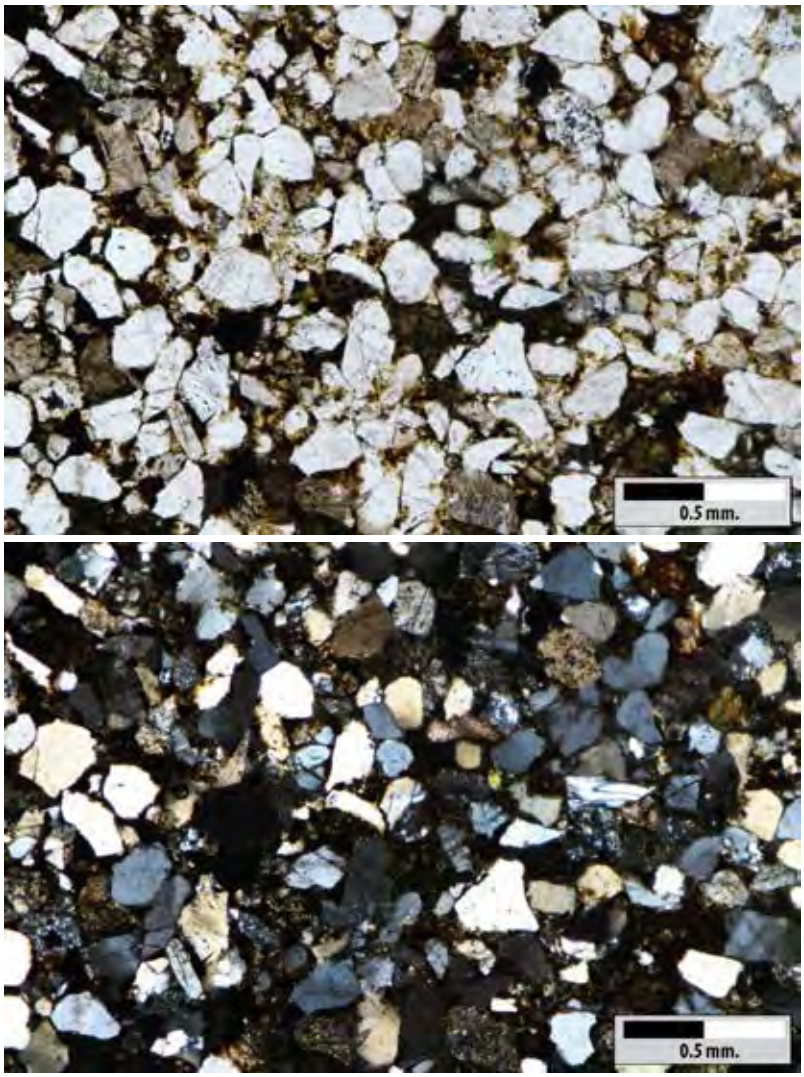

Figure 3.22 Thin-section of sample B at host rock (Top) PPL (Bottom) XPL (5X)

Mineral	Amount	
Quartz	112	0.44
Feldspar	62	0.24
Rock fragment	62	0.24
Opaque minerals	11	0.04
Mica	8	0.04
	255	1

Table 18 Amount of minerals in thin-section of sample B at host rock

Chapter 4

Discussion

4.1 ITRAX XRF core scanning data

To observe relationship of each element, coefficient correlation (r) and principle component analysis methods were used in this study. On coefficient correlation method, negative number means elements have opposite relations, zero number means no relations, and positive number means elements have a same way on relationship.

On coefficient correlation (r), Table 1 and Table 2 shows values from sample A, Table 3 and Table 4 for sample B of integral number of elements (i.e. Si, Fe, Al, K, and Ca) compare with each other. In this study, we focus on r values (0.700 <r< -0.700). Thus, relationship of main elements has been observed as follow;

Similarly, the results of principle component analysis can be also explained. Mono plot graph can display on figure 3.7 which is from sample A that Silicon (Si), Aluminium (Al), and Potassium (K) are positively correlated and also with Iron (Fe). On the other hand, Iron (Fe) shows correlation that dissimilarity with Silicon (Si), Aluminium (Al), and Potassium (K). While Calcium (Ca) seems to has non-correlation with the other elements.

Principle component analysis on the sample B is also correlated with positive relationship of Silicon (Si), Aluminium (Al), and Potassium (K) (Fig. 3.8). Conversely, Iron (Fe) shows contrast similar to PCA of sample A. But only Calcium (Ca) in this sample is non-correlated with the others.

Based on elemental data of sample A and B, it can be divide into three parts; first on the host rock, there is rich-elements of Silicon (Si), Aluminium (Al), Potassium (K) and has low contents of Iron (Fe), and Calcium (Ca). The second part called

"*Ophiomorpha nodosa* zone" is found increasing of Iron (Fe), and Calcium (Ca) instantly and the rich-elements on the host rock are decreased instead. The last one is called "Burrow fill" that is similar composition to the host rock but it has a little difference of elemental contents that are lower. On the sample B, Calcium (Ca) content in "*Ophiomorpha nodosa* zone" is decreased conversely but high content of Calcium (Ca) on "Burrow fill" instead. Also, the surrounding rock is similar in elemental compositions compare to sample A.

4.2 Conventional XRF elemental compositions

After Itrax XRF core scanning method were analyzed, we found that there are composed of three zones; the host rock, *Ophiomorpha nodosa*, and Burrow fill. Thus, we use conventional wavelength-dispersive X-ray fluorescence method for analyzing selected points where are associated with those zones. On results of both sample A and sample B found that the surrounding rock zone is composed of chemical concentration approximate to burrow fill zone (high SiO_2, K_2O, and Al_2O_3). While in *Ophiomorpha* zone SiO_2, K_2O, and Al_2O_3 decreases, but high contents of Fe_2O_3, and CaO.

4.3 Petrography and mineral identification

Thin-section is used for method to observe petrology of samples and X-ray diffraction method for mineralogy identification from d-spacing properties. We still observe three zones under polarized-light microscope and do point counting method in order to relate rock name with Folk's diagram. Classification based on the relative abundances of quartz (Q), feldspar (F), and rock fragments (R) (Folk, 1980).

In thin-section analysis, material in both burrow fill and the host rock zone are grain supported while *Ophiomorpha nodosa* zone is matrix supported. Furthermore, we found that grain compaction on sample A is closer than sample B. Considering on

zone of *Ophiomorpha*, there is difference of grain-to-grain that sample B has more spacing.

Grains were counted and plotted on Folk's ternary diagram both samples are grouped as Feldspathic-litharenite (Fig. 4.1). Similarly, method of X-ray diffraction is represented of Quartz-rich (more than 50 %). Moreover, *Ophiomorpha nodosa* zone of both sample A and sample B display peak of goethite (FeO(OH)) that we can assume that the presence of high content of Iron (Fe).

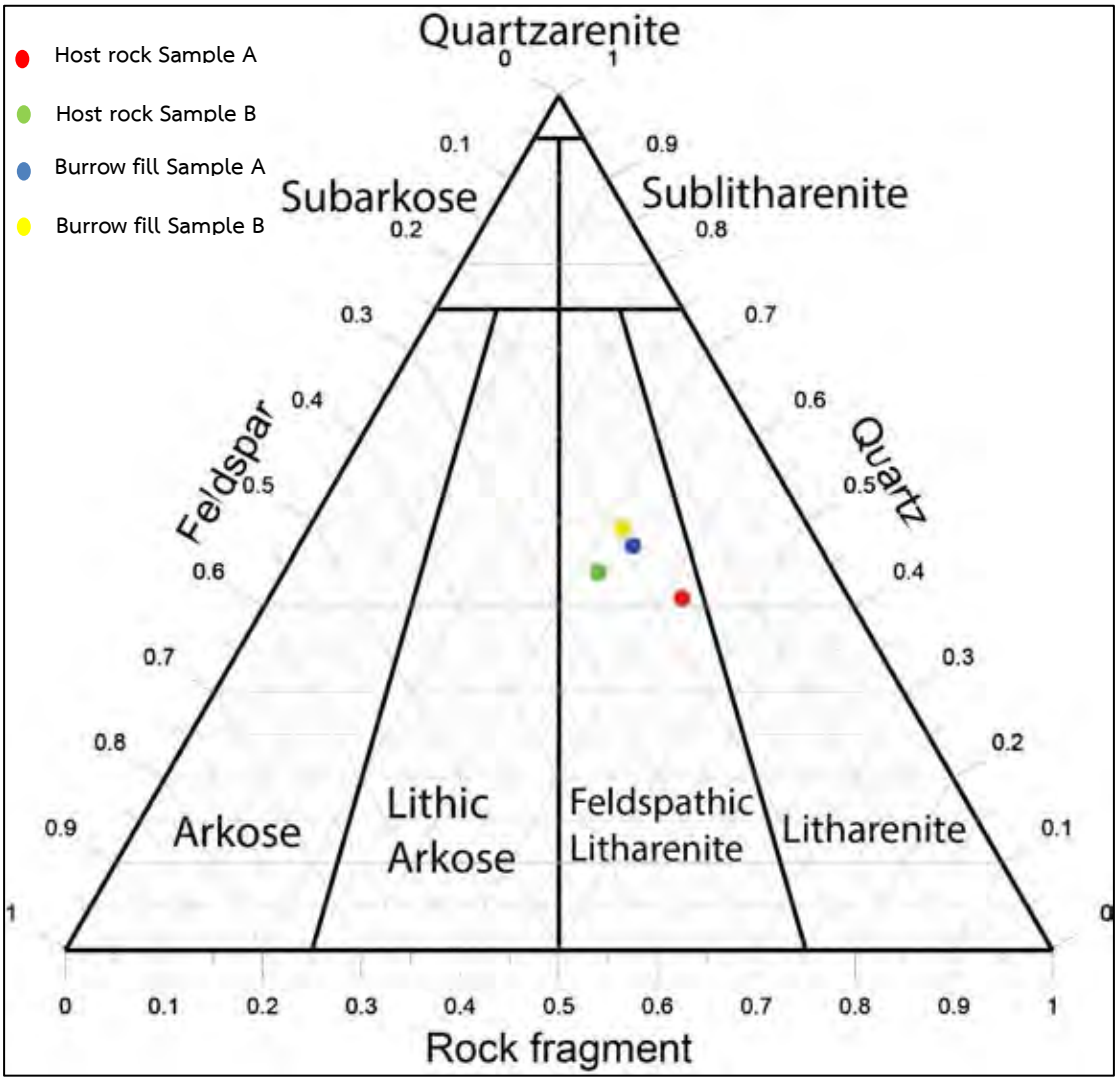

Figure 4.1 shows ternary diagram from point counting method (modified from Folk, 1980).

The study of petrography and XRD analysis are compared with the previous work (Löwemark et al., 2016) that have studied *Ophiomorpha* in other Formations, northeast coast of Taiwan. Petrography has well sorted, angular to sub-round grains and Quartz is the most grain. In XRD analysis, there is a similarity of *Ophiomorpha* that compose of Quartz, Feldspar and Goethite. Also, zones of host rock and burrow fill are composed of Quartz, Feldspar and the presence of mica (glauconite).

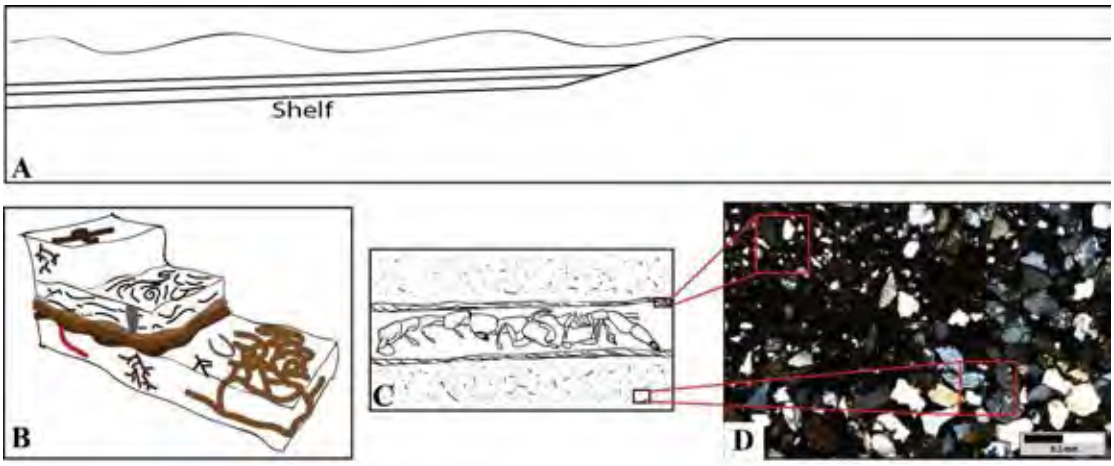

Figure 4.2 shows model of preliminary interpretation of paleoenvironment in the study area.

The presence of glauconite (Iron composed mica group) in sedimentary rock can be inferred that paleoenvironment in this study area is marine setting, commonly associated with low-oxygen condition. Glauconite is an indicator of shelf environment (Harden, 1980), and it can be formed by consequence of diagenesis of sedimentary deposits with low temperature. In this study, host rock is a part of Miocene sandstone, Nangang Formation that deposits on transgressive period (Fig. 4.2A). Furthermore, *Ophiomorpha* and other trace fossil (Fig. 4.2B) dominated while sediments were forming that can change decreasingly compaction of sediments around burrows (Fig.4.2C). Then, iron solution can fill during or after lithification. In other hand, Goethite was also found that can be inferred oxidizing condition (Kämpf and Schwertmann, 1983) after the sedimentary rock was exposed by tectonic setting or sea level change. It changes into subaerial condition (high oxygen) and iron can be oxidized to form

goethite. Fig. 4.2D the different petrography of boundary between *Ophiomorpha nodosa* zone and host rock zone shows the different grain size and grain compaction. On the field study, there are two different features (epilief and hyporelief) can be discussed that there is no difference in chemical composition but epirelief has more grain compaction compare with hyporelief under microscope of thin-section. It may be caused by ethological explanations that epirelief was formed in order to shelter thus it more densely in grain compaction. In contrast, deposit feeding, storage of material, or pathway can form other features as hyporelief.

Chapter 5

Conclusion

In this study, the rock samples were collected on the surface in the same sedimentary succession in order to compare the differential appearance on *Ophiomorpha nodosa* that aligns horizontally in along the surface of the host rock. These samples are separated in two features; epirelief and hyporelief due to the comparison of resistance between the host rock.

Based on elemental analysis and mineralogy on thin-section petrography, our samples are composed of high contents of Silicon (Si), Iron (Fe), Aluminium (Al) and Potassium (K) that can be formed SiO_2, $FeO(OH)$, $KAlSiO_2$ on mineralogy. Also, Feldspathic- litharenite is grouped by Folk's ternary diagram on both sample A (epirelief) and sample B (hyporelief).

According to elemental composition, the presence of high iron (Fe) content in *Ophiomorpah nodosa* zone in both samples, which mean the resistance of the trace fossil is not dependent on chemical composition due to the result of XRF and XRD of both samples show the same way. In addition, thin-section method displays differential matrix compaction between grains which epirelief (Sample A) is more grains of quartz and grain-supported that may compose cement of high iron (Fe) content (Goethite). It can be concluded that the difference in grain compaction between sample A and sample B due to the result of ethological explanations (i.e. behavior of organism or different usage of burrows).

These results can be concluded that the study of petrography is one of factors that play the important role for different erosion of *Ophiomorpha nodosa* and the host rock in the study area. There are still other factors that need to be consider e.g. difference in morphology and ichnospecies of the trace fossil *Ophiomorpha* in the same succession, or structural control.

Recommendation for further study

On the northeast coast of Taiwan is common with *Ophiomorpha nodosa* and other trace fossils that can be study for depositional environments, taxonomy, and mineralogy. In the field observation, there are a lot of interesting things that can be studied in the future such as a peculiar features of host rock, or fracture system controls on the sedimentary successions and many more. Furthermore, we hope to study more factors that might control the different features in this area.

References

วัฒนา ตันเสถียร. 2549. ร่องรอยสัตว์ดึกดำบรรพ์ในประเทศไทย. กรุงเทพฯ : สำนักธรณีวิทยา กรมทรัพยากรธรณี.

Bromley, Richard G., Robert, and W. Frey. N.d. Redescription of the Trace Fossil Gyrolitres and Taxonomic Evaluation of Tralassinoides, Opriomorpha and Spongeliomorpha.

Bromley, Richard G., and Ulla Asgaard. 1991. Ichnofacies: A Mixture of Taphofacies and Biofacies. Lethaia 24(2): 153–163.

CENTRAL GEOLOGICAL SURVEY, MOEA. N.d. https://www.moeacgs.gov.tw/english/twgeol/twgeol_introduction.jsp, accessed May 14, 2018.

Ekdale, A. A., and T. R. Mason. 1988. Characteristic Trace-Fossil Associations in Oxygen-Poor Sedimentary Environments. Geology 16(8): 720–723.

Folk Classification. 2018. Wikipedia. https://en.wikipedia.org/w/index.php?title=Folk_classification&oldid=822226680, accessed March 14, 2018.

Frey, Robert W., James D. Howard, and Wayne A. Pryor. 1978. Ophiomorpha: Its Morphologic, Taxonomic, and Environmental Significance. Palaeogeography, Palaeoclimatology, Palaeoecology 23(Supplement C). Trace Fossils and Their Importance in Paleoenvironmental Analysis: 199-229.

Frey, Robert W., S. George Pemberton, and Thomas D. A. Saunders. 1990. Ichnofacies and Bathymetry: A Passive Relationship. Journal of Paleontology 64(1): 155–158.

Harder, H. 1980. Syntheses of Glauconite at Surface Temperatures. Clays and Clay Minerals 28(3): 217–222.

Herreid, Clyde F., and Charles A. Gifford. 1963. The Burrow Habitat of the Land Crab, Cardisoma Guanhumi (Latreille). Ecology 44(4): 773–775.

Ho, C. S. 1986. A Synthesis of the Geologic Evolution of Taiwan. Tectonophysics 125(1). Geodynamics of the Eurasia\3-Philippine Sea Plate Boundary: 1–16.

Ian Croudace, and Guy Rothwell. 2010. Micro-XRF sediment core scanners: important new tools for the environmental and earth sciences. SPECTROSCOPYEUROPE: 6–13.

Kämpf, N., and U. Schwertmann. 1983. Goethite and Hematite in a Climosequence in Southern Brazil and Their Application in Classification of Kaolinitic Soils. Geoderma 29(1): 27–39.

Krajewski, K. P. 1984. Early Diagenetic Phosphate Cements in the Albian Condensed Glauconitic Limestone of the Tatra Mountains, Western Carpathians. Sedimentology 31(4): 443–470.

Löwemark, Ludvig, Yu-Chen Zheng, Subarna Das, Chung-Ping Yeh, and Tzu-Tung Chen. 2016. A Peculiar Reworking of Ophiomorpha Shafts in the Miocene Nangang Formation, Taiwan. Geodinamica Acta 28(1–2): 71–85.

Netto, Renata G., H. Allen Curran, Zain Belaústegui, and Francisco M. W. Tognoli. 2017. Solving a Cold Case: New Occurrences Reinforce Juvenile Callianassids as the Ophiomorpha Puerilis Tracemakers. Palaeogeography, Palaeoclimatology, Palaeoecology 475(Supplement C): 93–105.

Seilacher, Adolf. 1967. Bathymetry of Trace Fossils. Marine Geology 5(5). Depth Indicators in Marine Sedimentary Environments: 413–428.

Uchman, Alfred. 2009. The Ophiomorpha Rudis Ichnosubfacies of the Nereites Ichnofacies: Characteristics and Constraints. Palaeogeography, Palaeoclimatology, Palaeoecology 276(1): 107–119.